Reliable Computation of High Pressure Solid-Fluid Equilibrium

Gang Xu,[1] Aaron M. Scurto,[1] Marcelo Castier,[2]

Joan F. Brennecke,[1] and Mark A. Stadtherr*[1]

[1]Department of Chemical Engineering, 182 Fitzpatrick Hall,
University of Notre Dame, Notre Dame, IN 46556, USA

[2]Escola de Química, Universidade Federal do Rio de Janeiro,
Rio de Janeiro, RJ 21949-900, Brazil

August 1999
(revised, October 1999)

*Author to whom all correspondence should be addressed. Fax: (219) 631-8366; E-mail: markst@nd.edu

Abstract

The calculation of solid-fluid equilibrium at high pressure is important in the modeling and design of processes that use supercritical fluids to selectively extract solid solutes. We describe here a new method for reliably computing solid-fluid equilibrium at constant temperature and pressure, or for verifying the nonexistence of a solid-fluid equilibrium state at the given conditions. Difficulties that must be considered include the possibility of multiple roots to the equifugacity conditions, and multiple stationary points in the tangent plane distance analysis done for purposes of determining global phase stability. Somewhat surprisingly, these issues are often not dealt with by those who measure, model and compute high pressure solid-fluid equilibria, leading in some cases to incorrect or misinterpreted results. It is shown here how these difficulties can be addressed by using a methodology based on interval analysis, which can provide a mathematical and computational guarantee that the solid-fluid equilibrium problem is correctly solved. The technique is illustrated with several example problems in which the Peng-Robinson equation of state model is used. However, the methodology is general purpose and can be applied in connection with any model of the fluid phase.

Keywords: Phase Equilibrium, Phase Stability, Solid-Fluid Equilibrium, Supercritical Fluid Extraction, Interval Analysis

1 Introduction

In this paper we present a completely reliable technique, based on interval analysis, to compute solid-fluid equilibrium. The calculation of solid-fluid equilibrium is important in the modeling and design of processes that use supercritical fluids (SCFs) to selectively extract solid solutes, as, for example, in the decaffeination of coffee with supercritical CO_2.[1] The tunable solvent properties of SCFs, achieved with simple variations of temperature or pressure, make them attractive for extractions. Other commercial and research applications of SCF extraction include the ROSE process for the upgrading of petroleum residuals, the extraction of a variety of natural products, and the removal of radioactive and heavy metals from contaminated solid matrices.[1–3] Of increasing importance is the use of supercritical CO_2 as a replacement solvent for hazardous organic solvents in a variety of reaction systems, in which some of the components may be solids.[4] Supercritical CO_2, in particular, has been identified as an attractive environmentally benign solvent since it is non-toxic, non-flammable and inexpensive, and it has easily accessible critical properties (T_c = 304.2 K, $P_c = 73.76$ bar). Primarily over the last four decades, there have been extensive measurements of solid-fluid equilibria, so substantial data are available.[1,5] Nevertheless, to take advantage of the attractive attributes of SCFs in any type of process design, the physical properties and phase behavior of these solutions need to be modeled and computed accurately.

For process design calculations, supercritical fluid solutions are modeled almost exclusively with equation of state (EOS) models due to their simplicity, flexibility and ability to capture the correct temperature and pressure dependence of the density and all density-dependent properties, such as solubility.[1,6,7] Even the simple van der Waals equation can, at least qualitatively, describe most of the types of binary fluid behavior, as classified by von Konynenburg and Scott.[8] Probably the two most popular models are the Peng-Robinson equation[9] and the Soave-Redlich-Kwong equation.[10] These models generally require at least one binary interaction parameter, k_{ij}, that must be regressed from experimental data, to provide quantitative representation of the solubilities. More complicated EOS models (e.g., SAFT[11,12]) and mixing rules (e.g., Wong-Sandler[13] and Huran-Vidal[14]) with a stronger theoretical basis have been developed that, in many cases, do a better job than the simple cubic EOS models with standard mixing rules, but may require the use of more adjustable parameters.

Whether determining the best-fit k_{ij} from experimental data, or calculating the solubility of a solid at new conditions using a particular EOS model, there are two computational pitfalls that can be encountered in the calculation of solid-fluid equilibrium:

1. Solid solubilities in SCFs are usually computed by locating a mole fraction which satisfies the equifugacity equation relating the solute fugacity in the supercritical fluid, as predicted by the EOS, and the fugacity of the pure solid (see section 3.1 for further details). However, at certain values of temperature, pressure, and k_{ij}, there can exist multiple solutions to the equifugacity condition. A common method for solving the equifugacity equation is successive substitution or some similar approach,[1] using some small value of the solid solubility in the fluid phase as the initial guess. In general, this strategy will only find the smallest solubility root and may miss any larger values, if present, that satisfy the equifugacity equation. Thus, what is needed is a completely reliable method to determine *all* the roots to the equifugacity equation.

2. Equifugacity is a necessary but not sufficient condition for stable solid-fluid equilibrium. Solutions to the equifugacity equation must be tested for global thermodynamic phase stability. There are two widely used techniques to determine phase stability. One method is to examine the magnitude and sign of the appropriate determinants of partial derivatives;[15] this method can distinguish the unstable case from the stable or metastable cases, but cannot distinguish stable from metastable. The other method is based on tangent plane analysis;[16] this method can distinguish the stable case from the metastable or unstable cases, but cannot distinguish metastable from unstable. Since we are interested in determining the thermodynamically stable solutions to the equifugacity equations, we use tangent plane analysis here (see section 3.2 for further details). Tangent plane analysis itself, however, presents a difficult computational problem, which again can be addressed by using a completely reliable equation solving technique.

In this paper we address both of these computational issues, presenting a completely reliable method for determining all the solutions to the equifugacity equation, and then using a method that can test those solutions for stability with complete certainty. Thus, we present a methodology that is guaranteed to identify the correct, thermodynamically stable composition of a fluid phase in equilibrium with a pure solute.

2 Background

In order to understand the situations in which multiple solubility roots to the equifugacity equation are likely to exist, and for which stability analysis is particularly important, as well as to facilitate later discussion of results, it is useful to review the typical phase behavior of solvent-solute systems at high pressure.

The pressure-temperature projection of a typical binary solvent-solute system is shown in Fig. 1. This diagram shows a projection of all the salient features in the P-T-composition diagram. The solid line at low temperatures is the vapor pressure curve of the pure solvent, ending with a circle at the critical point (c.p.) of the pure fluid (e.g., CO_2). The solid lines at higher temperatures represent the sublimation curve, the vapor pressure curve (and critical point), and melting curve of the pure solute (e.g., naphthalene). In the presence of the solvent, the melting curve of the solute can be depressed, which is represented by the dashed-dotted SLV curve (solid, liquid and vapor in equilibrium) emanating from the triple point of the solute. This depression occurs because, for example, CO_2 that can dissolve in liquid naphthalene acts as an impurity, lowering the melting point of the naphthalene. This SLV line terminates in an upper critical end point (UCEP), indicated by a triangle, where the vapor and liquid phases become identical in the presence of the solid phase. The UCEP and the c.p. of the solute are connected by a dotted vapor-liquid critical line. Each point along that curve represents the temperature and pressure at which vapor and liquid phases become identical at different overall compositions ranging from pure naphthalene to the UCEP composition. Solid-liquid-vapor equilibrium can also occur at lower temperatures, as shown in the figure. This SLV line terminates at the lower critical end point (LCEP), where again the vapor and liquid phases become identical in the presence of the solid phase. The c.p. of the fluid and the LCEP are also connected by a vapor-liquid critical line.

At temperatures and pressures on the SLV lines, there are necessarily multiple solubility roots to the equifugacity equation, indicating equilibrium between the solid and a vapor at one solubility root, and between the solid and a liquid at another solubility root. In general, there is a significant range of temperatures and pressures around the SLV conditions for which there are also multiple solubility roots, only one of which is stable. Supercritical fluid extraction processes are usually operated at temperatures within about 50 °C of the pure fluid c.p., so that the separation can take advantage of the high compressibility of the fluid this close to the c.p. If the UCEP is within this range of investigation for operating conditions, then the possibility of solid-liquid-vapor equilibria exists, and we are in a range of temperature and pressure for which multiple roots are likely. Thus, the difficulty of multiple roots to the equifugacity equations is especially a problem when the melting point of the solid is not significantly greater than the c.p. of the fluid. Moreover, if one operates too close to the c.p. of the pure fluid, going below the LCEP, one may also observe solid-liquid-vapor equilibrium, and again be in a range of temperature and pressure for which multiple solubility roots are likely.

The detailed phase behavior at five different temperatures is shown in Figs. 2–6. Fig. 2 shows schemat-

ically a pressure-composition diagram at T_{A}, a temperature below the c.p. of the solvent. At very low pressures, one would have just vapor mixtures across the entire overall composition range. At higher pressures and at feed compositions of the solute greater than its solubility limit in the vapor phase, one would observe solid-vapor equilibrium. At the pressure indicated by the SLV line, all three phases would exist over a very wide feed composition range: the pure solid at point **a**, a liquid with a composition indicated by point **b**, and a vapor with a composition indicated by point **c**. At pressures just above the SLV line, the number of phases present depends on the overall feed composition. Feeds rich in the solute would result in solid-liquid equilibrium. Feeds that are mostly CO_2 would be single-phase vapor. Feeds of intermediate concentrations could be either a single-phase liquid or vapor-liquid equilibrium. The vapor-liquid envelope is connected at the pure solvent side of the diagram at its vapor pressure at T_{A}. Above this pressure, one would observe either solid-liquid equilibrium or a single liquid phase. At this temperature, there is a wide range of pressure for which multiple solubility roots will be observed, below the SLV line including a stable solid-vapor root and metastable solid-liquid root, and above the SLV line including a stable solid-liquid root and a metastable solid-vapor root.

At temperatures between the c.p. of the fluid and the LCEP (e.g., T_{B}), the pressure-composition diagram (Fig. 3) looks very similar to that at lower temperatures, except that the vapor-liquid envelope has detached from the left-hand side of the plot. This is because the temperature is above the c.p. of CO_2, so it no longer has a pure component vapor pressure. Thus, the vapor-liquid dome now comes together at its top in a mixture critical point, which corresponds to the dotted line between the c.p. of CO_2 and the LCEP in Fig. 1. At the temperature of the LCEP, the solid-vapor, solid-liquid and vapor-liquid regions merge into a single solid-fluid equilibrium region, as seen in Fig. 4 for temperature T_{C}. The curve exhibits the characteristic inflection point at the LCEP, where the solid solubility in the fluid increases dramatically with a small increase in pressure. At temperatures between the LCEP and the UCEP (Fig. 5, temperature T_{D}), the system is either single-phase or exhibits solid-fluid equilibria. The diagram is qualitatively similar to that at the LCEP, except that the solute solubility increase in the fluid phase as a function of pressure is much more gradual. At the UCEP, an inflection like at the LCEP reappears, signaling the reformation of a liquid phase. Multiple solubility roots over some pressure interval are possible for some range of temperature above the LCEP, and for some range below the UCEP; however, for systems with a wide temperature gap between the LCEP and UCEP, there will also be a wide range of temperatures in this gap for which there is only a single solubility root to the equifugacity condition at all pressures of interest. At temperatures above the UCEP (Fig. 6, temperature T_{E}), the diagram is qualitatively similar to temperatures between the c.p. of CO_2 and

the LCEP (Fig. 3).

In the design of a supercritical extraction process in which the solute melting point is close to the c.p. of the solvent, there will not be a large gap between the LCEP and UCEP. In this case, the range of operating temperatures that should be considered range from temperatures like T_{B} to those like T_{E}, and thus will include a significant range for which there are multiple solubility roots. In some cases, the low solubility (solid-vapor) root will be the correct one, but in other cases solid-liquid or even solid-liquid-vapor equilibrium may exist. Although many such systems exist, the most frequently studied system that exhibits solid-liquid and solid-liquid-vapor equilibria at normal operating conditions is the one already mentioned, namely CO_2 and naphthalene (melting temperature of 80.5 °C).[17] There are significant amounts of experimental data available for this system.[18–22] A dynamic flow apparatus, where the fluid flows slowly over a bed packed with the solid, and then is analyzed, is commonly used for these measurements. However, as noted by McHugh and Yogan,[21] and later reconfirmed by Chung and Shing,[22] these measurements may actually yield the composition of the vapor in equilibrium with a liquid phase, not the composition of the fluid phase in equilibrium with a pure solid. As explained in Example 3 below, failure to correctly determine the stable solid-fluid root to the equifugacity condition may make it difficult to detect when this occurs, thus leading to the misinterpretation of vapor-liquid data as solid-fluid data, as happened to McHugh and Paulaitis.[20] Thus, care in measurement, modeling and computation is vitally important for these types of systems.

Somewhat surprisingly, the practice of searching for all roots to the equifugacity condition and testing for phase stability appears not to be widespread among those who measure, model and compute high pressure solid-fluid equilibria. However, the need to test for stability and its influence on phase diagrams has been an area of interest to some researchers. For example, Hong et al.[23] mapped out the phase diagrams for a variety of binary systems, including CO_2/naphthalene, using the Peng-Robinson EOS with standard (van der Waals) mixing rules. They apparently identified the equifugacity roots graphically, using plots of fugacity vs. composition. Nitta et al.[24] mapped out phase diagrams using the Soave-Redlich-Kwong EOS. They did phase stability analysis using the tangent plane approach, and employed the algorithm developed by Michelsen.[25] While this is generally a very reliable algorithm, it is a local, initialization-dependent method, and is known to yield incorrect results in some situations.[26] More recently, Wisniak et al.[27] used a modified van der Waals EOS and standard mixing rules to predict gas-solid phase behavior including both the solvent-rich LCEP and solute-rich UCEP. They used a successive substitution technique to solve the equifugacity equation, with a marching-type approach to aid in initializing the calculation. Other work, notably that of Marcilla et al.,[28] has focused on low-pressure solid-liquid equilibrium, and the need for careful stability

analysis in that context as well. These researchers[23,24,27] were able to carefully map out the full phase diagrams for their selected systems. However, the computational methods they used are local, initialization-dependent solvers, which in general provide no guarantee that all equifugacity roots are found, nor that phase stability analysis is done correctly. In this paper, we present a technique that *does* provide these guarantees, and thus can determine *with certainty* the correct, stable solution to the solid-fluid equilibrium problem. The technique is based on interval analysis, which has previously been applied to a variety of difficult problems in the modeling of phase behavior.[26,29–31] Here we show how it can be applied to the completely reliable solution of solid-fluid equilibrium problems.

3 Problem Formulation

Consider a solvent-solute system in which the solute (component 2) may be present in a pure solid phase in equilibrium with a single fluid phase in which the solvent (components 1,3,...C) is present. It is desired to compute, from appropriate thermodynamic models, the solubility (mole fraction) y_2 of the solute in the fluid phase at specified temperature, pressure, and overall composition. As discussed above, this problem presents a number of computational difficulties.

3.1 Equifugacity Condition

The standard formulation of this problem is based on the equifugacity condition for the solute; that is, assuming an equation-of-state (EOS) model for the fluid phase,

$$f_2^{\mathrm{S}}(T,P) = \hat{f}_2^{\mathrm{F}}(T,P,\mathbf{y},v), \tag{1}$$

where f_2^{S} is the fugacity of the solute in the pure solid phase, $\hat{f}_2^{\mathrm{F}}$ is fugacity of the solute in the fluid phase solution, $\mathbf{y} = (y_1, y_2, \ldots, y_C)^{\mathrm{T}}$ is the vector of fluid phase mole fractions, and v is the molar volume of the fluid from the EOS model. Additional relationships that must be satisfied are the summation to one of the fluid phase mole fractions

$$\sum_{i=1}^{C} y_i = 1 \tag{2}$$

and the EOS for the fluid phase $P = \mathcal{F}_{\mathrm{P}}(T,\mathbf{y},v)$, which here is assumed to be the Peng-Robinson EOS.

$$P = \mathcal{F}_{\mathrm{P}} = \frac{RT}{v-b} - \frac{a(T)}{v(v+b)+b(v-b)}. \tag{3}$$

Standard (van der Waals) mixing rules will be used, namely $a = \sum_i \sum_j y_i y_j a_{ij}$ and $b = \sum_i y_i b_i$. Here $a_{ii}(T)$ and b_i are pure component parameters computed from the critical temperature, critical pressure, and acentric factor for pure component i, and $a_{ij} = \sqrt{a_{ii} a_{jj}}(1 - k_{ij})$, with k_{ij} representing a binary interaction parameter. Values of k_{ij} obtained by fit to experimental data frequently vary somewhat with T.

The fugacity of solute in the pure solid phase can be expressed as[32]

$$f_2^{\mathrm{S}}(T, P) = P_2^{\mathrm{sub}}(T)\phi_2^{\mathrm{sub}}(T) \exp\left[\frac{v_2^{\mathrm{S}}}{RT}(P - P_2^{\mathrm{sub}}(T))\right]$$

where $P_2^{\mathrm{sub}}(T)$ is the sublimation pressure at the system temperature T, $\phi_2^{\mathrm{sub}}(T)$ is the fugacity coefficient of the pure vapor in equilibrium with the solid at T and $P_2^{\mathrm{sub}}(T)$, and v_2^{S} is the molar volume of the pure solid. The exponential term on the right hand side is the Poynting correction factor, assuming that v_2^{S} is constant. Since $P_2^{\mathrm{sub}}(T)$ is likely to be small, it is also assumed that $\phi_2^{\mathrm{sub}}(T) = 1$. Note that, at specified constant T and P, f_2^{S} is a constant. The fugacity of the fluid phase can be written as

$$\hat{f}_2^{\mathrm{F}}(T, P, \mathbf{y}, v) = y_2 P \hat{\phi}_2^{\mathrm{F}}(T, P, \mathbf{y}, v),$$

where the fugacity coefficient $\hat{\phi}_2^{\mathrm{F}}$ of the solute in the fluid phase solution can be determined from the EOS.[32]

There are also material balance considerations. On a solute-free basis, the solvent composition is constant and assumed specified by the given mole fractions $\xi_i, i \neq 2$. In terms of ξ_i, the independent material balances on the solvent species are

$$y_i = \xi_i(1 - y_2), \quad i = 3, \ldots, C. \tag{4}$$

Eqs. (1–4) form a system of $C + 1$ equations in the $C + 1$ variables $\mathbf{y}$ and v.

A common approach for solving this equation system is to note that from Eq. (4) for $y_i, i = 3, \ldots, C$ and Eq. (2) for y_1, it is clear that the composition of the fluid phase, and thus from Eq. (3) its molar volume, can be treated as a function of y_2 only. Thus, the equifugacity relationship can be stated as

$$y_2 = \frac{P_2^{\mathrm{sub}}(T)}{P\hat{\phi}_2^{\mathrm{F}}(T, P, y_2)} \exp\left[\frac{v_2^{\mathrm{S}}}{RT}(P - P_2^{\mathrm{sub}}(T))\right]$$

and, at specified T and P, solved iteratively for y_2 by a successive substitution scheme, with a typical initial guess being some small value of solubility, such as $y_2^{(0)} = P_2^{\mathrm{sub}}/P$.

As discussed above, a major difficulty in solving this problem is that the equation system to be solved, namely Eqs. (1–4), may have multiple solutions. Furthermore, since the equifugacity equation is a necessary but not sufficient condition for equilibrium, any solution found must be tested for stability. These issues will be discussed in more detail in the next section.

An additional issue is that the solute material balance imposes a constraint on y_2. If the specified overall mole fraction of solute is ψ_2 and the molar solid phase fraction at equilibrium is s, then the solute material balance is $\psi_2 = s + y_2(1-s)$ or $y_2 = (\psi_2 - s)/(1-s)$. From this it follows that $0 \leq y_2 \leq \psi_2$. If there is no solution of Eqs. (1–4) that satisfies this constraint, then there is no solid phase at equilibrium. As emphasized by Bullard and Biegler,[33] the presence of such constraints in a nonlinear equation solving problem can be problematic.

An approach to equation solving that can deal rigorously with all these issues, namely the potential for multiple solutions, the need for a stability test, and the constraint that $y_2 \in [0, \psi_2]$, is the use of interval analysis, as demonstrated below.

3.2 Stability Analysis

For a fluid-fluid equilibrium problem at constant temperature and pressure, it is well known that a solution to the equifugacity condition can be interpreted as the tangent points on a plane tangent to the Gibbs energy surface of the fluid. However, if this plane ever crosses (goes above) the Gibbs energy surface, then this indicates that the phases represented by the tangent points are not stable, and that this is not the solution to the phase equilibrium problem.

For a solid-fluid equilibrium problem, the geometric interpretation is similar,[28] but there are important differences:

1. Since only one fluid phase is assumed, there will in general be only *one* point of tangency to the Gibbs energy curve of the fluid.

2. The pure solid phase is represented by a single *point*, at composition $y_2 = 1$ and Gibbs energy g_2^{S}, where g_2^{S} indicates the (molar) Gibbs energy of the pure solid phase relative to a pure fluid phase at the given temperature and pressure, and can be determined from $g_2^{\mathrm{S}} = RT \ln(f_2^{\mathrm{S}}/f_2^{\mathrm{F}})$. Both the solid phase fugacity f_2^{S} and fluid phase fugacity f_2^{F}, can be determined as described in Section 3.1, and are constant at constant T and P. Thus, the point representing the solid is fixed by the given T and P.

3. A solution to the equifugacity equation can be interpretated as a tangent to the curve representing the fluid phase that goes through the point representing the pure solid phase. As in the fluid-fluid case, if this tangent ever goes above the Gibbs energy surface, then this solution to the equifugacity condition does not represent a stable phase equilibrium.

This is shown schematically for several cases in Figs. 7–10, using a hypothetical plot of the Gibbs energy of mixing g_{m} for the fluid phase versus solubility y_2. In Fig. 7, there is only one possible tangent to the Gibbs energy curve that goes through the solid point (1, g_2^{S}). In this case, there will be only one solution to Eqs. (1–4). Fig. 8 shows a case in which there will be three solutions, indicated by the three tangent lines that also pass through the solid point (1, g_2^{S}). Two of these lines cross the Gibbs energy curve and represent solutions that are not stable. The line tangent at the lowest value of y_2 gives the stable solution. Fig. 9 also shows a case with three solutions, except in this case it is the line tangent at the highest value of y_2 that gives the stable solution. Finally, Fig. 10 shows a case in which there again are three solutions, however two of them lie on the same tangent line. Since this tangent does not cross the Gibbs energy curve, this indicates that there are two stable solutions, at the tangent points with the highest and lowest y_2 values. This represents the special case of solid-liquid-vapor equilibrium.

The determination of phase stability is often done using the concept of tangent plane distance.[16,25] The tangent plane distance D is simply the distance from the tangent plane to the Gibbs energy of mixing surface. That is,

$$D(\mathbf{y}, v) = g_{\mathrm{m}}(\mathbf{y}, v) - g_{\mathrm{m}}(\mathbf{y_0}, v_0) - \sum_{i=1}^{C} \left(\frac{\partial g_{\mathrm{m}}}{\partial y_i}\right)_0 (y_i - y_{i0})$$

where the subscript zero indicates evaluation at one of the points of tangency $\mathbf{y_0}$ satisfying the equifugacity condition. If D ever becomes negative, then the tangent has crossed the Gibbs energy surface and the phase being tested is not stable. A common approach for determining if D is ever negative is to minimize D and check the sign of its minimum. This minimization is done subject to the mole fractions summing to one and subject to the equation of state relating $\mathbf{y}$ and v. Using a Lagrangian approach, it can be easily shown that the stationary points in this optimization problem must satisfy

$$\left[\left(\frac{\partial g_{\mathrm{m}}}{\partial y_i}\right) - \left(\frac{\partial g_{\mathrm{m}}}{\partial y_C}\right)\right] - \left[\left(\frac{\partial g_{\mathrm{m}}}{\partial y_i}\right) - \left(\frac{\partial g_{\mathrm{m}}}{\partial y_C}\right)\right]_0 = 0, \qquad i = 1, \ldots, C-1 \tag{5}$$

For the Peng-Robinson EOS, expressions for g_{m} and $\partial g_{\mathrm{m}}/\partial y_i$ are given by Hua et al.[34] and others.

Eqs. (2), (3) and (5) form a $(C+1) \times (C+1)$ system of equations that can be solved for the stationary points of D. This equation system has a trivial root at $\mathbf{y} = \mathbf{y}_0$ and $v = v_0$ and may have multiple nontrivial roots as well, corresponding to multiple stationary points in D. If any stationary point corresponds to a value of D less than zero, then the conclusion is that the phase represented by $\mathbf{y}_0$ is not stable. If *all* the stationary points are found and *all* have a nonnegative D, meaning that the global minimum of D is zero (at $\mathbf{y} = \mathbf{y}_0$), then the conclusion is that the phase is stable. However, without a *guarantee* that *all* stationary points of D have been found, or equivalently that the *global* minimum of D has been found, incorrect conclusions could

be drawn. For example, if one stationary point of D is missed when solving the equation system, and that is the only stationary point for which D is negative, then based on the other stationary points found, one would conclude that the phase was stable, when in fact it is not stable.

In the context of fluid-fluid equilibrium, the problem of reliable phase stability analysis has attracted much interest.[35–37] However, for equation-of-state models, only the approach of Hua et al.,[26,34,38] based on interval analysis, and the more recent work, based on a branch-and-bound global optimization method, of Harding and Floudas[39] provide a guarantee that the correct conclusion is reached. Here we will use the interval approach to phase stability analysis in the context of solid-fluid equilibrium.

4 Solution Method

4.1 Interval Analysis

We apply here interval mathematics, in particular an interval Newton/generalized bisection (IN/GB) technique, to find, or, more precisely, to find very narrow enclosures of, all solutions of a nonlinear equation system, or to demonstrate that there are none. Recent monographs which introduce interval computations include those of Neumaier,[40] Hansen[41] and Kearfott.[42] The algorithm used here has been described by Hua et al.,[26] and given in more detail by Schnepper and Stadtherr.[43] Properly implemented, this technique provides the power to find, *with mathematical and computational certainty*, enclosures of *all* solutions of a system of nonlinear equations,[40,42] or to determine with certainty that there are none, provided that initial upper and lower bounds are available for all variables. This is made possible through the use of the powerful existence and uniqueness test provided by the interval Newton method. The technique can also be used to determine with certainty the *global* minimum of a nonlinear objective function. Our implementation of the IN/GB method for solid-fluid equilibrium problem is based on appropriately modified routines from the FORTRAN-77 packages INTBIS[44] and INTLIB.[45] The key ideas of the methodology used are summarized very briefly here.

Consider the solution of a nonlinear equation system $\mathbf{f}(\mathbf{z}) = \mathbf{0}$ where $\mathbf{z} \in \mathbf{Z}^{(0)}$ (interval quantities are indicated in upper case, point quantities in lower case). The solution algorithm is applied to a sequence of intervals, beginning with the initial interval vector $\mathbf{Z}^{(0)}$ specified by the user. This initial interval can be chosen to be sufficiently large to enclose all physically feasible behavior, or to represent some constraint given in the problem. For an interval $\mathbf{Z}^{(k)}$ in the sequence, the first step in the solution algorithm is the *function range test*. Here an *interval extension* $\mathbf{F}(\mathbf{Z}^{(k)})$ of the function $\mathbf{f}(\mathbf{z})$ is calculated. An interval

extension provides upper and lower bounds on the range of values that a function may have in a given interval. It is often computed by substituting the given interval into the function and then evaluating the function using interval arithmetic. The interval extension so determined is often wider than the actual range of function values, but it always includes the actual range. If there is any component of the interval extension $\mathbf{F}(\mathbf{Z}^{(k)})$ that does not contain zero, then we may discard the current interval $\mathbf{Z}^{(k)}$, since the range of the function does not include zero anywhere in this interval, and thus no solution of $\mathbf{f}(\mathbf{z}) = \mathbf{0}$ exists in this interval. Otherwise, if zero is contained in $\mathbf{F}(\mathbf{Z}^{(k)})$, then processing of $\mathbf{Z}^{(k)}$ continues.

The next step is to apply the *interval Newton test* to the current interval $\mathbf{Z}^{(k)}$. This involves setting up and solving a system of linear interval equations for a new interval, the *image* $\mathbf{N}^{(k)}$. Comparison of the current interval and the image provides a powerful existence and uniqueness test.[40,42] If $\mathbf{N}^{(k)}$ and $\mathbf{Z}^{(k)}$ have a null intersection, then this is mathematical proof that there is no solution of $\mathbf{f}(\mathbf{z}) = \mathbf{0}$ in $\mathbf{Z}^{(k)}$. If $\mathbf{N}^{(k)}$ is a proper subset of $\mathbf{Z}^{(k)}$, then this is mathematical proof that there is a *unique* solution of $\mathbf{f}(\mathbf{z}) = \mathbf{0}$ in $\mathbf{Z}^{(k)}$. If neither of these two conditions is true, then no conclusions can be made about the number of solutions in the current interval. However, it is known[46] that any solutions that do exist must lie in the intersection of $\mathbf{N}^{(k)}$ and $\mathbf{Z}^{(k)}$. If this intersection is sufficiently smaller than the current interval, one can proceed by reapplying the interval Newton test to the intersection. Otherwise, the intersection is bisected, and the resulting two intervals added to the sequence of intervals to be tested. These are the basic ideas of an interval Newton/generalized bisection (IN/GB) method.

It should be emphasized that, when machine computations with interval arithmetic operations are done, as in the procedures outlined above, the endpoints of an interval are computed with a directed outward rounding. That is, the lower endpoint is rounded down to the next machine-representable number and the upper endpoint is rounded up to the next machine-representable number. In this way, through the use of interval, as opposed to floating point, arithmetic any potential rounding error problems are eliminated. Overall, the IN/GB method described above provides a procedure that is mathematically *and* computationally guaranteed to enclose all solutions to the nonlinear equation system or to determine with certainty that there are none.

4.2 Computing Solid-Fluid Equilibrium

In applying the method outlined above to the solid-fluid equilbrium problem, the first step is to establish an initial interval in which to search for solutions to the equifugacity condition, Eqs. (1–4). To do this, the material balance constraint $0 \leq y_2 \leq \psi_2$ is used. Thus the initial interval for y_2 is $Y_2^{(0)} = [0, \psi_2]$. Initial

intervals for the remaining components of $\mathbf{y}$ can then be determined using Eqs. (2) and (4), using interval arithmetic. The initial interval for v is taken to have the lower limit of $v_{\min} = \min_i b_i$, and the upper limit of $2RT/P$ (compressibility factor of 2); that is, $V^{(0)} = [\min_i b_i, 2RT/P]$.

The IN/GB algorithm is now applied to the simultaneous solution of Eqs. (1–4), thus determining with certainty *all* the roots of the system of equations within the given initial interval, or determining with certainty that there are none. In the latter case, this is mathematical proof that there is no solid phase present at equilibrium. Note that if a conventional local solver were used, and it converged, for several initial guesses, to a $y_2 > \psi_2$, it might be tempting to conclude that there was no solid phase; however, this could not be done with certainty since there could still be an untried initial guess for which a $y_2 < \psi_2$ might be found. The IN/GB approach is essentially initialization independent, requiring not an initial point guess, but an initial interval, which can be chosen to represent all physically feasible behavior, not some guess.

The next step is to begin testing the equifugacity roots, just found, for stability. This requires solving the system of Eqs. (2), (3) and (5), in which $\mathbf{y}_0$ is one of the equifugacity roots. Again this is done using the IN/GB algorithm, thus guaranteeing that all the stationary points of the tangent plane distance D, or equivalently, the global minimum of D, are found. It should be noted[26] that, in the context of tangent plane analysis, the IN/GB algorithm can be implemented in combination with a simple branch and bound scheme, so that intervals containing stationary points that cannot be the global minimum of D are eliminated and, thus, all stationary points of D need not be enclosed. For this problem, each mole fraction has the initial interval [0,1] and the initial volume interval is the same as used in the equifugacity problem. If the global minimum of D is zero, then the equifugacity root being tested represents a stable phase, and the solution to the solid-fluid equilibrium problem has been found. Otherwise, the phase being tested is not stable, and so the next equifugacity root is tested. If after all roots are tested for stability, none are stable, this indicates that the assumption of solid-fluid equilibrium is not correct. For the given solute feed ψ_2 there may be fluid-fluid equilibrium, or there may be solid-fluid-fluid equilibrium. Note that the conclusion that there is no solid-fluid equilibrium cannot be made with certainty in this way unless one is certain that *all* equifugacity roots have been found, a guarantee that is provided when the interval method is used.

One special case should be noted, namely the case of a *binary* system for which $\psi_2 \to 1$ (this indicates the assumption of an inexhaustible supply of solute). In this case: 1. If there is a unique solution to the equifugacity condition then it must be stable (see Fig. 7). 2. If there are multiple equifugacity roots, one of them must be stable and it corresponds to the one with the lowest tangent (see Figs. 8 and 9); i.e., the one with the lowest $g_{\rm m}$ at any fixed value of $y_2 < 1$, say at $y_2 = 0$. Alternatively (and equivalently), this stable

root can be identified by choosing the one at which the total Gibbs energy of the system (solid and fluid) is the lowest. Thus, for this special case, the tangent plane distance analysis for stability can be bypassed. However, in the examples below, since we want to test the performance of the most general form of the methodology, even in problems for which a large solute loading ($\psi_2 \rightarrow 1$) is assumed in a binary system, we will perform the tangent plane analysis rather than bypass it.

5 Results and Discussion

Using the method described in Section 4, and the Peng-Robinson EOS, we have calculated the solubility of caffeine, anthracene, naphthalene, and biphenyl in CO_2, and the solubility of anthracene in a fluid mixture of ethane and CO_2. These example systems are representative of the types of systems that may be encountered in supercritical fluid extraction. They include cases where there is only one root to the equifugacity equation, as well as where there are multiple roots. We use interval methods to identify all roots to the equifugacity equation, as well as to test for phase stability, with complete certainty.

The values of the critical properties, acentric factors, and pure solute molar volumes used in each example are given in Table 1. Solute sublimation pressures $P_i^{\rm sub}(T)$ are computed from $\log_{10} P_i^{\rm sub}(T) = A_i - (B_i/T)$. Here $P_i^{\rm sub}$ has units of Pa and T has units of K. Values of the constants A_i and B_i are given in Table 1. Unless otherwise noted, the entire composition space was searched for equifugacity roots; that is, we allowed $\psi_2 \rightarrow 1$, which is equivalent to assuming that there is an infinite amount of solid solute available in the system. Computations were done on a Sun Ultra 10/440 workstation. The CPU time required ranges from about 0.15 to 0.65 seconds for solving the equifugacity condition, and from about 0.2 to 6 seconds for the stability analysis, with the larger times on the ternary system in Example 5. These computation times are much higher than what is required by the local, but possibly unreliable, methods typically used in the context of solid-fluid equilibrium. Thus, there is a choice between fast methods that may give the wrong answer, or this slower method that is guaranteed to give the correct answer.

5.1 Example 1: Caffeine/CO_2

The solubility of caffeine in supercritical CO_2 has been the focus of much research, eventually leading to the construction of commercial plants to extract caffeine from tea and coffee.[1,4] Here we compute the solubility of caffeine in CO_2 at 313.15 K, 333.15 K and 353.15 K and pressures to 350 bar. The binary interaction parameter, k_{12}, that is needed in the Peng-Robinson EOS was chosen to give the best fit of the

experimental data,[47] at each temperature. The values used were $k_{12} = -0.0675$ at 313.15 K, -0.080 at 333.15 K, and -0.095 at 353.15 K.

Using the IN/GB method, we determined that there was only one root to the equifugacity equation at each of the temperatures and pressures considered. Though the stability analysis could have been safely bypassed in this case, as described in the discussion of the special case in Section 4.2, we nevertheless, for the sake of generality, tested the single equifugacity root at each T and P for phase stability using the interval tangent plane method described above, and confirmed that the phase was stable.

The results are shown in Fig. 11. Here the open symbols represent computed roots of the equifugacity equation at each of the three temperatures; for clarity, here and in the subsequent examples, the roots are plotted only at selected pressures. The solid line indicates the complete set of stable solutions. (Throughout this section we will use open symbols to indicate roots of the equifugacity condition, in general only some of which will be stable, and a solid line to indicate those roots that correspond to a stable phase.) There is only one root to the equifugacity equation at each T and P considered in this example because the operating conditions (313.15, 333.15 and 353.15 K) chosen are well below the melting point of caffeine (511.15 K).[17] Therefore, all temperatures investigated are well below the UCEP. Moreover, none of the temperatures are very close to the c.p. of CO_2 so it is apparent that all temperatures investigated are between the LCEP and the UCEP. As a result, we predict solid-fluid equilibria at all conditions investigated. The predicted values match experimental measurements of solid-fluid equilibria for this system very well but those data are not included on the graph for the sake of clarity.

5.2 Example 2: Anthracene/CO_2

This example involves the binary system of anthracene/CO_2 at 308.15 K and 328.15 K. The k_{12} value used at both temperatures was $k_{12} = 0.0675$, based on a fit to the experimental solid-fluid equilibria data of Johnston et al.[48] The computed results are shown schematically in Fig. 12. This system is very similar to the caffeine/CO_2 system in that there is only one root to the equifugacity equation at each temperature and pressure investigated, as shown by the open symbols in Fig. 12. Since the entire composition space was searched for roots, as was done for caffeine/CO_2, these roots are the stable ones, as indicated by the solid lines on the graph. As a result, this system exhibits simple solid/fluid equilibria at all conditions investigated. It is reasonable to expect only solid-fluid equilibria for this system since the melting point of anthracene is 489.15 K,[17] well above the temperatures of interest.

5.3 Example 3: Naphthalene/CO_2

As mentioned in Section 2, naphthalene/CO_2 is a system that exhibits very rich high pressure phase behavior. Moreover, it is one of the most widely studied SCF systems and one for which some of the earliest solid-fluid equilibrium data is available.[18] The normal melting point of naphthalene is 80.5 °C (353.65 K)[17] and it exhibits significant melting point depression in the presence of CO_2, yielding a UCEP around 60.1 °C (333.25 K).[21,49]

The results of solving the equifugacity condition and performing the phase stability test using the interval method for naphthalene/CO_2 at 308.15 K are shown in Fig. 13. Like in the anthracene/CO_2 system, at this temperature there is only one root to the equifugacity equation at every pressure and that root is the correct, stable solubility. Based on this information, we can conclude that 308.15 K is between the LCEP and the UCEP of this system. The k_{12} used at this temperature was $k_{12} = 0.095$, based on a fit to the solid-fluid equilibrium data of McHugh and Paulaitis.[20]

Fig. 14 shows the computed results at 328.15 K. Here, unlike in the anthracene/CO_2 case at this T, for a range of pressures up to about 310 bar, multiple roots to the equifugacity condition were found using the interval approach, as indicated by the open circles on the plot. Using the interval tangent plane analysis to test phase stability at these roots, we found that the lowest solubility roots were always the stable ones. Thus, the solid line in Fig. 14, indicating stable solid-fluid equilibrium, is very similar to that in Fig. 13 for the 308.15 K case. It can be concluded that this temperature is still below the UCEP, as has been shown experimentally.[21,49] At this temperature, we used $k_{12} = 0.0974$, again based on fit to the solid-fluid equilibrium data of McHugh and Paulaitis,[20] which is shown on the plot by solid triangles.

At 338.05 K, with the same k_{12} used at 328.15 K ($k_{12} = 0.0974$), multiple roots to the equifugacity equation are also obtained over a wide range of pressures, as shown in Fig. 15. Using the interval phase stability test, we were able to identify the correct, stable solutions. At this temperature, however, the lowest solubility root does not always correspond to a stable phase. At low pressure, the low solubility root is the correct result, indicating solid-vapor or solid-fluid equilibrium. However, at about 73.60 bar, both the lowest solubility root and the highest solubility root are stable, indicating solid-liquid-vapor equilibrium; that is, a pure solid phase in equilibrium with a vapor phase containing less than a tenth of a percent of naphthalene and a liquid phase containing more than 60 mol% naphthalene. This pressure is reasonably close to the experimentally observed SLV line, which is found at about 80 bar.[49] At pressures above this three phase line, the naphthalene-rich liquid phase is the stable root, and so solid-liquid equilibrium will exist, as long as the initial loading ψ_2 of naphthalene is sufficiently high. At even higher pressures, there is only one (high

solubility) root to the equifugacity equation, representing the liquid phase in equilibrium with the solid. The set of stable roots is shown by the solid curve in Fig. 15. Clearly, 338.05 K is above the UCEP for the naphthalene/CO_2 system and the phase diagram resembles that shown schematically in Figure 6.

Also shown in Fig. 15 are the experimental data of McHugh and Paulaitis[20] at this temperature. They originally reported these data as representing solid-fluid equilibrium. Clearly, however, according to the Peng-Robinson model, the values that they reported do not correspond to the stable phase in equilibrium with the solid, which would be required to have a composition of greater than 50 mol% naphthalene. As acknowledged later,[21] these measurements were actually the composition of a vapor phase in equilibrium with a *liquid*—there was no solid present. However, since there was no visual observation of the sample, the researchers did not realize that they were operating at a temperature above the UCEP, which was not measured until later.[21,49] To replicate computationally the experiments of McHugh and Paulaitis, we performed a calculation at 338.05 K and 150 bar, in which we specified $\psi_2 = 0.05$ instead of $\psi_2 \to 1$; that is, a relatively small initial loading of solute. In this case, because of the solute material balance constraint $y_2 \in [0, \psi_2]$, when we solve the equifugacity condition we only find one root (at $y_2 = 0.0182$), and when that root is tested for stability, we find that it does not correspond to a stable phase. This indicates, with certainty, that the model does not predict solid-fluid equilibrium. In modeling this system, we would have to now discard the assumption that a solid phase is present, and instead look for stable vapor-liquid equilibrium. This was done using an interval-based, completely reliable flash routine that has been discussed previously.[50] The results of these vapor-liquid equilibrium calculations at a variety of pressures are shown by the dashed curve in Fig. 15. The data of McHugh and Paulaitis that was thought to be solid-fluid, but which actually is not, matches the composition of a vapor phase (predicted from the Peng-Robinson equation) in equilibrium with a naphthalene-rich liquid phase relatively well. This was confirmed with the experimental data of Chung and Shing,[22] who measured the vapor-liquid equilibrium of this system at this temperature using a visual cell. This vapor-liquid equilibria corresponds to the VLE envelope shown schematically in Fig. 6.

As one additional computational experiment at this temperature, we considered the the specification of 150 bar and $\psi_2 = 0.0001$, an extremely small solute loading. In this case, using the interval approach to solve the equifugacity condition, we found, that there were no roots, thus indicating with certainty that there was no solid phase present at equilibrium. At these conditions, this mixture is stable as a single fluid phase, corresponding to a point in the vapor phase region to the left of the VLE envelope in Fig. 6.

There are two very important points to be made from this example. First, experimentalists must be very careful to look for the presence of liquid phases when attempting to measure solid-fluid equilibria. If optical

cells are not available, they should model the phase behavior at higher temperatures, perhaps using the best-fit k_{12} at a lower temperature where they are sure they are safely in the solid-fluid equilibrium region. Then, in computing the phase behavior at the higher temperature, they must be careful to find *all* roots (not just the lowest solubility root) to the equifugacity equation and to use a completely reliable method, such as the one presented here, to test for phase stability. Second, modelers must be very careful to ascertain that their model actually predicts the correct phase behavior for the system of interest. For instance, at 328.15 K, and using $k_{12} = 0.095$, instead of the value $k_{12} = 0.0974$ used to compute Fig. 15, an SLV line is predicted at about 153 bar, but only solid-fluid equilibria is observed experimentally. In this case, the lowest solubility root might match the experimental solid-fluid data quite well, but this model would be incorrect because the lowest solubility root is not stable at pressures above the SLV line. Thus if one looks only for one solubility root and fails to do phase stability analysis, one might incorrectly assume that he or she had established a good model of the system.

The last temperature that we examine for this system is at 304.25 K, just above the c.p. of pure CO_2, where we use $k_{12} = 0.095$. This is the value that fit the experimental data at 308.15 K, which, as shown above, is safely in the solid-fluid region. The roots to the equifugacity equation at this temperature are shown by the open circles in Fig. 16, where the region between about 72.2 and 73.2 bar is enlarged in the inset. For a very small pressure range there are three roots to the equifugacity equation, as shown in the inset. At pressures below about 72.825 bar, the lowest solubility root is stable, indicating solid-fluid equilibria. At about 72.825 bar, both the lowest and highest solubility roots are stable, indicating solid-liquid-vapor equilibria. As is the case at 338.05 K, at higher pressures, the highest solubility root is the stable one, indicating solid-liquid equilibria. Thus, this is a temperature between the c.p. of the CO_2 and the LCEP. Qualitatively, the phase diagram for this system corresponds to that shown in Fig. 3 (temperature T_{B} in Figure 1).

5.4 Example 4: Biphenyl/CO_2

The melting point of biphenyl is 344.15 K,[17] again close to the c.p. of CO_2, and this is another system for which experimental data has been mistakenly reported as solid-fluid equilibrium,[20] but later identified as actually vapor-liquid equilibrium.[21]

The results for this system at 308.15 K are shown in Fig. 17. At this temperature, there is only one equifugacity root (open circle) at each pressure, and these are stable (solid line). This indicates solid-fluid equilibrium only, so this temperature is between the LCEP and the UCEP, just as is the case for naphthalene

at this same temperature. Here we used $k_{12} = 0.08$, based on a fit to data of Chung and Shing.[22]

Using the same $k_{12} = 0.08$ determined at 308.15 K, the Peng-Robinson equation predicts that this system can form a liquid phase at 333.15 K. As shown in Fig. 18, at this temperature there are three roots to the equifugacity equation over a wide range of pressures (assuming $\psi_2 \to 1$). At low pressures the interval tangent plane analysis correctly identifies the lowest solubility root as stable. At about 45.19 bar, both the lowest and highest roots are stable, indicating solid-liquid-vapor equilibrium, and at higher pressures the high solubility root is the stable one, indicating solid-liquid equilibrium. This is entirely equivalent to the naphthalene/CO_2 system at 338.05K. The model shows that this temperature must be above the UCEP and, indeed, visual observations of this system indicate the UCEP is at 328.25 K.[21]

5.5 Example 5: Anthracene/CO_2/Ethane

The interval techniques for solving the equifugacity condition and testing for phase stability are also applicable to multicomponent systems. Here we provide an example in which we compute the solubility of anthracene in a mixture of CO_2 and ethane at 308.15 K. The composition of the solvent on a solute-free basis was taken to be $\xi_1 = 5/6$ for CO_2, and $\xi_3 = 1/6$ for ethane. The binary interaction parameters used were determined from binary data: $k_{12} = 0.0675$ (anthracene/CO_2),[48] $k_{23} = 0.0225$ (anthracene/ethane),[48] and $k_{13} = 0.1322$ (ethane/CO_2 from the AspenPlus database). Since the melting point of anthracene (489.15 K)[17] is well above the operating temperature, we anticipate only solid-fluid equilibrium and this is what we observe, as shown in Figure 19 (at the system temperature, the phase diagram will be similar to that shown schematically in Figure 5, and there will be no vapor-liquid equilibrium). There is only one root to the equifugacity equation at each pressure investigated (again assuming $\psi_2 \to 1$). Moreover, the root at each pressure is stable, as determined from the interval tangent plane analysis for the ternary system. As discussed above in Section 4.2, if, in a binary system, there is only one equifugacity root across the whole composition range ($\psi_2 \to 1$), then testing for stability could be bypassed. However, with a mixed solvent, the phase stability test must be performed. This is because the original fluid mixture might be two phase (usually vapor-liquid) or the dissolution of the solute in the fluid mixture may induce a vapor-liquid phase split. This cannot be determined from the solid-fluid equifugacity equation, but would be identified during the tangent plane phase stability test, which would identify the solid/fluid equifugacity root as not stable. In such a case, the assumption of solid-fluid equilibrium would have to abandoned, and instead vapor-liquid, or solid-vapor-liquid equilibrium considered. However, in this example, the single root to the equifugacity equation at each pressure is indeed stable, as indicated on Fig. 19.

6 Concluding Remarks

We have described here a new method for reliably computing solid-fluid equilibrium at constant temperature and pressure, or for verifying the nonexistence of a solid-fluid equilibrium state at the given conditions. The method is based on interval analysis, in particular an interval Newton/generalized bisection algorithm, which provides a *mathematical and computational guarantee* that all roots to the equifugacity equation are enclosed, and that phase stability analysis is performed correctly. The guarantee of reliability comes at some cost in terms of computation time. Thus, one has a choice between fast methods that may give the wrong answer, or a slower method that is guaranteed to give the correct answer. In the work presented here, the fluid phase was modeled using a cubic EOS model, in particular the Peng-Robinson equation. However, the technique is general purpose and can be applied in connection with any model of the fluid phase. In addition to the solution of solid-fluid equilibrium problems, the methodology used here can also be applied to a wide variety of other problems in the modeling of phase behavior,[26,30,31,34,51] and in the solution of process modeling problems.[43]

Acknowledgements—This work has been supported in part by the Department of Energy Grant DE-FG07-96ER14691, the Environmental Protection Agency Grants R826-734-01-0 and R824-731-01-0, the National Science Foundation Grants CTS-9522835 and EEC97-00537-CRCD, and the donors of The Petroleum Research Fund, administered by the ACS, under Grant 30421-AC9. We also acknowledge the National Science Foundation for a supplement to CTS-952283 for Pan-American collaboration. GX acknowledges support from the University of Notre Dame as a Provost's Scholar. MC acknowledges the financial support of CNPq/Brazil and Pronex (Grant number 124/96).

References

(1) McHugh, M. A; Krukonis, V. J. *Supercritical Fluid Extraction: Principles and Practice*; Butterworth-Heinemann: Boston, 1990.

(2) Roggeman, E. J.; Scurto, A. M.; Stadtherr, M. A.; Brennecke, J. F. Spectroscopy, Measurement and Modeling of Metal Chelate Solubility in Supercritical CO_2. In *Proceedings of the 8th International Symposium on Supercritical Fluid Chromatography and Extraction*, St. Louis, MO, July 12-16, 1998.

(3) Laintz, K. E.; Wai, C. M.; Yonker, C. R.; Smith, R. D. Extraction of Metal Ions from Liquid and Solid Materials by Supercritical Carbon Dioxide. *Anal. Chem.* **1992**, *64*, 2875.

(4) Brennecke, J. F. New Applications of Supercritical Fluids. *Chem. Ind.–London*, Nov. 4, **1996**, No. 21, 831.

(5) Dohrn, R.; Brunner, G. High Pressure Fluid-Phase Equilibria–Experimental Methods and Systems Investigated (1988-1993). *Fluid Phase Equilib.* **1995**, *106*, 213.

(6) Johnston, K. P.; Peck, D. G.; Kim, S. Modeling Supercritical Mixtures–How Predictive Is It? *Ind. Eng. Chem. Res.* **1989**, 28, 1115.

(7) Brennecke, J. F.; Eckert, C. A. Phase Equilibria for Supercritical Fluid Process Design. *AIChE J.* **1989**, *35* 1409.

(8) van Konynenburg, P. H.; Scott, R. L. Critical Lines and Phase Equilibria in Binary van der Waals Mixtures. *Philos. Trans. R. Soc. London, Ser. A* **1980**, *298*, 495–540.

(9) Peng, S.Y.; Robinson, D. B. A New Two Constant Equation of State. *Ind. Eng. Chem. Fund.* **1976**, *8*, 766.

(10) Soave, G. Equilibrium Constants from a Modified Redlich-Kwong Equation of State. *Chem. Eng. Sci.* **1972**, *27*, 1197.

(11) Chapman, W. G.; Gubbins, K. E.; Jackson, G.; Radosz, M. SAFT—Equation-of-State Solution Model for Associating Fluids. *Fluid Phase Equilib.* **1989**, *52*, 31.

(12) Chapman, W. G.; Gubbins, K. E.; Jackson, G.; Radosz, M. New Reference Equation of State for Associating Liquids. *Ind. Eng. Chem. Res.* **1990**, *29*, 1709.

(13) Wong, D. S. H.; Sandler, S. I. A Theoretically Correct Mixing Rule for Cubic Equations of State. *AIChE J.* **1992**, *38*, 671.

(14) Huron, M.-J.; Vidal, J. New Mixing Rules in Simple Equations of State for Representing Vapour-Liquid Equilibria of Strongly Non-Ideal Mixtures. *Fluid Phase Equilib.* **1979**, *3*, 255.

(15) Beegle, B.L.; Modell, M.; Reid, R. C. Thermodynamic Stability Criterion for Pure Substances and Mixtures. *AIChE J.* **1974**, *20*, 1200.

(16) Baker, L. E.; Pierce, A. C.; Luks, K. D. Gibbs Energy Analysis of Phase Equilibria. *Soc. Petrol. Engrs. J.* **1982**, *22*, 731.

(17) Weast, R. C., Ed. *CRC Handbook of Chemistry and Physics*, 64th ed.; CRC Press: Boca Raton, Florida, 1983.

(18) Tsekhanskaya, Yu. V.; Iomtev, M. B.; Mushkina, E. V. Solubility of Naphthalene in Ethylene and Carbon Dioxide Under Pressure. *Russ. J. Phys. Chem.* **1964**, *38*, 1173.

(19) Najour, G. C.; King, A. D. Solubility of Naphthalene in Compressed Methane, Ethylene, and Carbon Dioxide. Evidence for a Gas-Phase Complex between Naphthalene and Carbon Dioxide. *J. Chem. Phys.* **1966**, *45*, 1915.

(20) McHugh, M.; Paulaitis, M. E. Solid Solubilities of Naphthalene and Biphenyl in Supercritical Carbon Dioxide. *J. Chem. Eng. Data* **1980** *25*, 326.

(21) McHugh, M. A; Yogan, T. J. Three-Phase Solid-Liquid-Gas Equilibria for Three Carbon Dioxide-Hydrocarbon Solid Systems, Two Ethane-Hydrocarbon Solid Systems, and Two Ethylene-Hydrocarbon Soid Systems. *J. Chem. Eng. Data* **1984**, *29*, 112.

(22) Chung, S. T.; Shing, K. S. Multiphase Behavior of Binary and Ternary Systems of Heavy Aromatic Hydrocarbons with Supercritical Carbon Dioxide. Part I. Experimental Results. *Fluid Phase Eq.* **1992**, *81*, 321.

(23) Hong, G. T.; Modell, M.; Tester, J. W. Binary Phase Diagrams from a Cubic Equation of State. In *Chemical Enginnering at Supercritical Conditions*; Paulaitis, M. E.; et al., Eds.; Ann Arbor Science: Ann Arbor, Michigan, 1982.

(24) Nitta, T.; Ikeda, K.; Katayama, T. Phase Equilibrium Calculations and Three-Dimensional Computer Graphics Representation. *Fluid Phase Equilib.* **1989**, *53*, 105.

(25) Michelsen, M. The Isothermal Flash Problem. Part I. Stability. *Fluid Phase Equilib.*,**1982** *9*, 1.

(26) Hua, J. Z.; Brennecke, J. F.; Stadtherr, M. A. Enhanced Interval Analysis for Phase Stability: Cubic Equation of State Models. *Ind. Eng. Chem. Res.* **1998**, *37*, 1519.

(27) Wisniak, J.; Apelblat, A.; Segura, H. Prediction of Gas-Solid Equilibrium using Equations of State. *Fluid Phase. Equilib.* **1998**, *147*, 45.

(28) Marcilla, A.; Conesa, J. A.; Olaya, M. M. Comments on the Problematic Nature of the Calculation of Solid-Liquid Equilibrium. *Fluid Phase Equilib.* **1997**, *135*, 169.

(29) Hua, J. Z.; Maier, R. W.; Tessier, S. R.; Brennecke, J. F.; Stadtherr, M. A. Interval Analysis for Thermodynamic Calculations in Process Design: A Novel and Completely Reliable Approach. *Fluid Phase Equilib.* **1999**, *158*, 607.

(30) Tessier, S. R.; Brennecke, J. F.; Stadtherr, M. A. Reliable Phase Stability Analysis for Excess Gibbs Energy Models. *Chem. Eng. Sci.* **1999**, in press.

(31) Maier, R. W., Brennecke, J. F.; Stadtherr, M. A. Reliable Computation of Homogeneous Azeotropes. *AIChE J.* **1998**, *44*, 1745.

(32) Prausnitz, J. M.; Lichtenthaler, R. N.; Gomes de Azevedo, E. *Molecular Thermodynamics of Fluid-Phase Equilibria*; Prentice-Hall: Englewood Cliffs, New Jersey, 1986.

(33) Bullard, L. G.; Biegler, L. T. Iterative Linear Programming Strategies for Constrained Simulation. *Comput. Chem. Eng.* **1991**, *15*, 239.

(34) Hua, J. Z.; Brennecke, J. F.; Stadtherr, M. A. Reliable Computation of Phase Stability Using Interval Analysis: Cubic Equation of State Models. *Comput. Chem. Eng.* **1998**, *22*, 1207.

(35) McDonald, C. M.; Floudas, C. A. Global Optimization for the Phase Stability Problem. *AIChE J.* **1995**, *41*, 1798.

(36) Sun, A. C.; Seider, J. D. Homotopy-Continuation Method for Stability Analysis in the Global Minimization of the Gibbs Free Energy. *Fluid Phase Equilib.* **1995**, *103*, 213.

(37) Wasylkiewicz, S. K.; Sridhar, L. N.; Malone, M. F.; Doherty, M. F. Global Stability Analysis and Calculation of Liquid-Liquid Equilibrium in Multicomponent Mixtures. *Ind. Eng. Chem. Res.* **1996**, *35*, 1395.

(38) Hua, J. Z.; Brennecke, J. F.; Stadtherr, M. A. Reliable Prediction of Phase Stability Using an Interval-Newton Method. *Fluid Phase Equilib.* **1996**, *116*, 52.

(39) Harding, S. T.; Floudas, C. A. Global Optimization Approach for the Phase and Chemical Equilibrium Problem using Equations of State. Presented at AIChE Annual Meeting, Miami Beach, Florida, November 15–20, 1998.

(40) Neumaier, A. *Interval Methods for Systems of Equations*; Cambridge University Press: Cambridge, England, 1990.

(41) Hansen, E. R.*Global Optimization Using Interval Analysis*; Marcel Dekkar: New York, 1992.

(42) Kearfott, R. B. *Rigorous Global Search: Continuous Problems*; Kluwer Academic Publishers: Dordrecht, The Netherlands, 1996.

(43) Schnepper, C. A.; Stadtherr, M. A. Robust Process Simulation Using Interval Methods. *Comput. Chem. Eng.* **1996**, *20*, 187.

(44) Kearfott, R. B.; Novoa, M. Algorithm 681: INTBIS, a Portable Interval Newton/Bisection Package. *ACM Trans. Math. Software* **1990**, *16*, 152.

(45) Kearfott, R. B.; Dawande, M.; Du, K.-S.; Hu, C.-Y. Algorithm 737: INTLIB, A Portable FORTRAN 77 Interval Standard Function Library. *ACM Trans. Math. Software* **1994**, *20*, 447.

(46) Moore, R. E. *Interval Analysis*, Prentice-Hall: Englewood Cliffs, New Jersey, 1966.

(47) Johannsen, M.; Brunner, G. Solubilities of the Xanthines Caffeine, Thephylline and Theobromine in Supercritical Carbon Dioxide. *Fluid Phase Equilib.* **1994**, *95*, 215.

(48) Johnston, K. P.; Ziger, D. H.; Eckert, C. A. Solubilities of Hydrocarbon Solids in Supercritical Fluids: The Augmented van der Waals Treatment. *Ind. Eng. Chem. Fundam.* **1982**, *21*, 191.

(49) Lamb, D. M.; Barbara, T. M.; Jonas, J. NMR Study of Solid Naphthalene Solubilities in Supercritical Carbon Dioxide Near the Upper Critical End Point. *J. Phys. Chem.* **1986**, *90*, 4210.

(50) Hua, J. Z.; Brennecke, J. F.; Stadtherr, M. A. Combined Local and Global Approach to Reliable Computation of Phase Equilibria. Presented at AIChE Annual Meeting, Los Angeles, CA, November 16–21, 1997.

(51) Gau, C.-Y.; Stadtherr, M. A. Nonlinear Parameter Estimation Using Interval Analysis. *AIChE Symp. Ser.* **1999**, *94*(320), 445.

(52) Li, S.; Varadarajan, G.S.; Hartland, S. Solubilities of Theobromine and Caffeine in Supercritical Carbon Dioxide: Correlation with Density-Based Models. *Fluid Phase Equilib.* **1991**, *68*, 263.

(53) Bothe, H.; Camenga, H. K. Phase Transitions and Thermodynamic Properties of Anhydrous Caffeine. *J. Therm. Anal.* **1979**, *16*, 267.

(54) Schmitt, W. J.; Reid, R. C. Solubility of Monofunctional Organic Solids in Chemically Diverse Supercritical Fluids. *J. Chem. Eng. Data* **1986**, *31*, 204.

(55) Reid, R. C.; Prausnitz, J. M.; Poling B. E. *The Properties of Gases and Liquids*, 4th ed.; McGraw-Hill: New York, 1987.

Table 1: Physical properties used in example problems.

compound	T_c (K)	P_c (bar)	ω	v^S (cc/mol)	A	B (K)
*Caffeine[52,53]	855.62	41.46	0.555	145.68	15.031	5781
Anthracene[54]	869.3	31.24	0.353	142.6	14.755	5313.7
Naphthalene[54]	748.4	40.5	0.302	111.4	13.583	3733.9
Biphenyl[54]	789.0	38.5	0.372	132.0	14.804	4367.4
Carbon Dioxide[54]	304.2	73.76	0.225			
Ethane[54]	305.4	48.8	0.098			

*For caffeine, the critical properties and acentric factor were estimated by the Joback group contribution approach, using parameters from Reid et al.[55]

Figure Captions

Figure 1. The pressure-temperature projection of a typical binary solvent-solute system. See text for discussion.

Figure 2. Pressure-composition diagram at temperature T_{A} in Figure 1. See text for discussion.

Figure 3. Pressure-composition diagram at temperature T_{B} in Figure 1. See text for discussion.

Figure 4. Pressure-composition diagram at temperature T_{C} in Figure 1. See text for discussion.

Figure 5. Pressure-composition diagram at temperature T_{D} in Figure 1. See text for discussion.

Figure 6. Pressure-composition diagram at temperature T_{E} in Figure 1. See text for discussion.

Figure 7. Hypothetical plot of Gibbs energy of mixing g_{m} vs. solubility y_2, showing a situation in which there is only one root to the equifugacity condition. g_2^{S} indicates the Gibbs energy of pure solid solute relative to pure fluid solute at the system temperature and pressure.

Figure 8. Hypothetical plot of Gibbs energy of mixing g_{m} vs. solubility y_2, showing a situation in which there are three roots to the equifugacity condition. Only the lowest solubility root represents a stable phase. g_2^{S} indicates the Gibbs energy of pure solid solute relative to pure fluid solute at the system temperature and pressure.

Figure 9. Hypothetical plot of Gibbs energy of mixing g_{m} vs. solubility y_2, showing a situation in which there are three roots to the equifugacity condition. Only the highest solubility root represents a stable phase. g_2^{S} indicates the Gibbs energy of pure solid solute relative to pure fluid solute at the system temperature and pressure.

Figure 10. Hypothetical plot of Gibbs energy of mixing g_{m} vs. solubility y_2, showing a situation in which there are three roots to the equifugacity condition. Here both the lowest and highest solubility roots represents stable phases, indicating solid-liquid-vapor equilibrium. g_2^{S} indicates the Gibbs energy of pure solid solute relative to pure fluid solute at the system temperature and pressure.

Figure 11. Computed equifugacity roots for Example 1, showing the solubility of caffeine in CO_2. There is only one equifugacity root at each temperature and pressure considered, and that root corresponds to stable solid-fluid equilibrium.

Figure 12. Computed equifugacity roots for Example 2, showing the solubility of anthracene in CO_2. There is only one equifugacity root at each temperature and pressure considered, and that root corresponds to stable solid-fluid equilibrium.

Figure 13. Computed equifugacity roots for Example 3, showing the solubility of naphthalene in CO_2 at 308.15 K. At this temperature, there is only one equifugacity root at each pressure considered, and that root corresponds to stable solid-fluid equilibrium.

Figure 14. Computed equifugacity roots for Example 3, showing the solubility of naphthalene in CO_2 at 328.15 K. At this temperature, there are multiple equifugacity roots for pressures below about 310 bar. The lowest solubility root always corresponds to stable solid-fluid equilibrium. Experimental data is from McHugh and Paulaitis.[20]

Figure 15. Computed equifugacity roots for Example 3, showing the solubility of naphthalene in CO_2 at 338.05 K. At this temperature, there are multiple equifugacity roots for pressures below about 170 bar. At low pressure the lowest solubility root corresponds to stable solid-fluid equilibrium, but at higher pressure it is the highest solubility root that is stable. A three-phase line (SLV) occurs at about 73.60 bar. The experimental data of McHugh and Paulaitis[20] was originally reported as solid-fluid, but clearly is not. See text for further discussion.

Figure 16. Computed equifugacity roots for Example 3, showing the solubility of naphthalene in CO_2 at 304.25 K. The portion of the curve enclosed in the box is enlarged in the inset to its right. At this temperature, there are multiple equifugacity roots for a small range of pressures between about 72.2 and 73.2 bar, with a three-phase line (SLV) at about 72.825 bar.

Figure 17. Computed equifugacity roots for Example 4, showing the solubility of biphenyl in CO_2 at 308.15 K. At this temperature, there is only one equifugacity root at each pressure considered, and that root corresponds to stable solid-fluid equilibrium.

Figure 18. Computed equifugacity roots for Example 4, showing the solubility of biphenyl in CO_2 at 333.15 K. At this temperature, there are multiple equifugacity roots for pressures below about 160 bar. At low pressure the lowest solubility root corresponds to stable solid-fluid equilibrium, but at higher pressure it is the highest solubility root that is stable. A three-phase line (SLV) occurs at about 45.19 bar.

Figure 19. Computed equifugacity roots for Example 5, showing the solubility of anthracene in a mixed solvent of 5:1 (molar) CO_2 and ethane at 308.15 K. At this temperature, there is only one equifugacity root at each pressure considered, and that root corresponds to stable solid-fluid equilibrium.

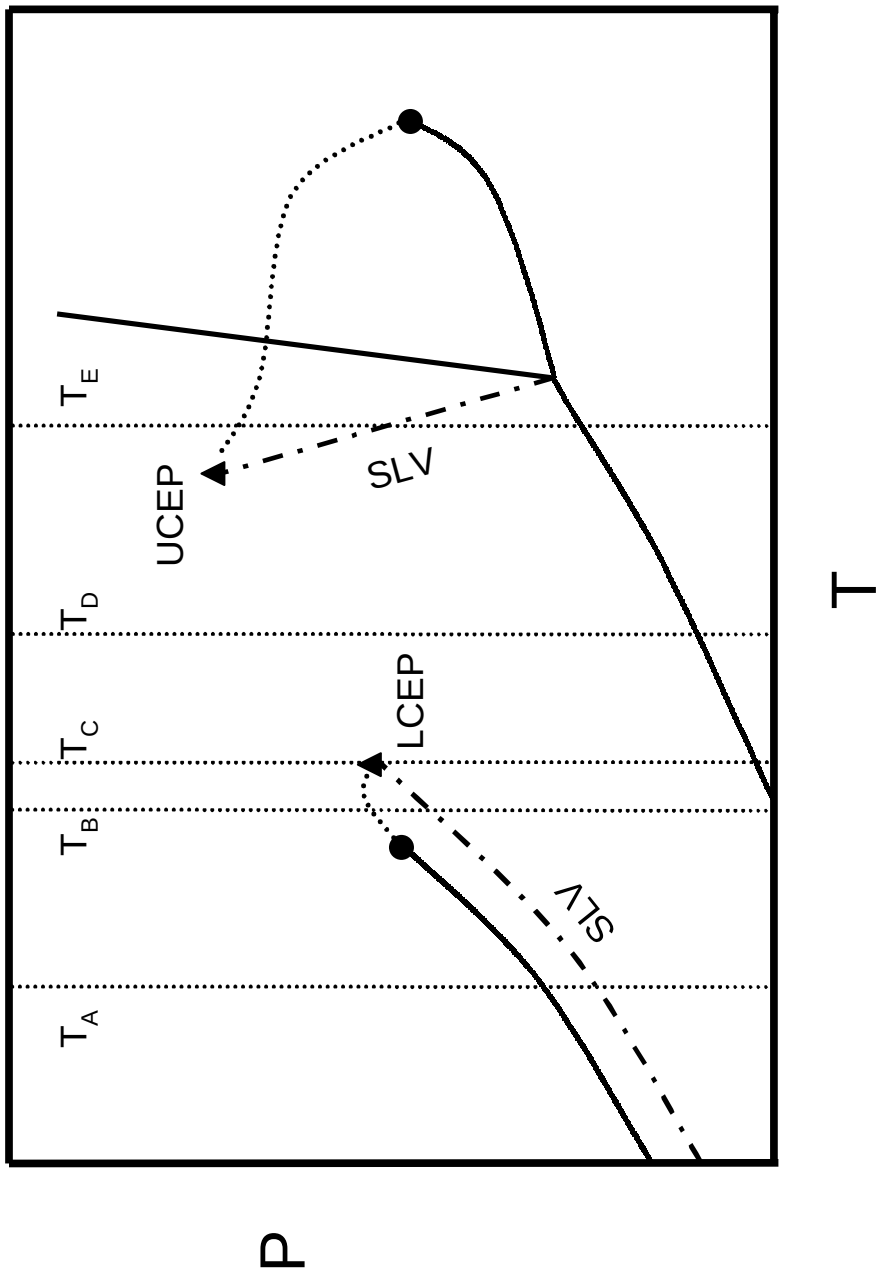

Figure 1: The pressure-temperature projection of a typical binary solvent-solute system. See text for discussion.

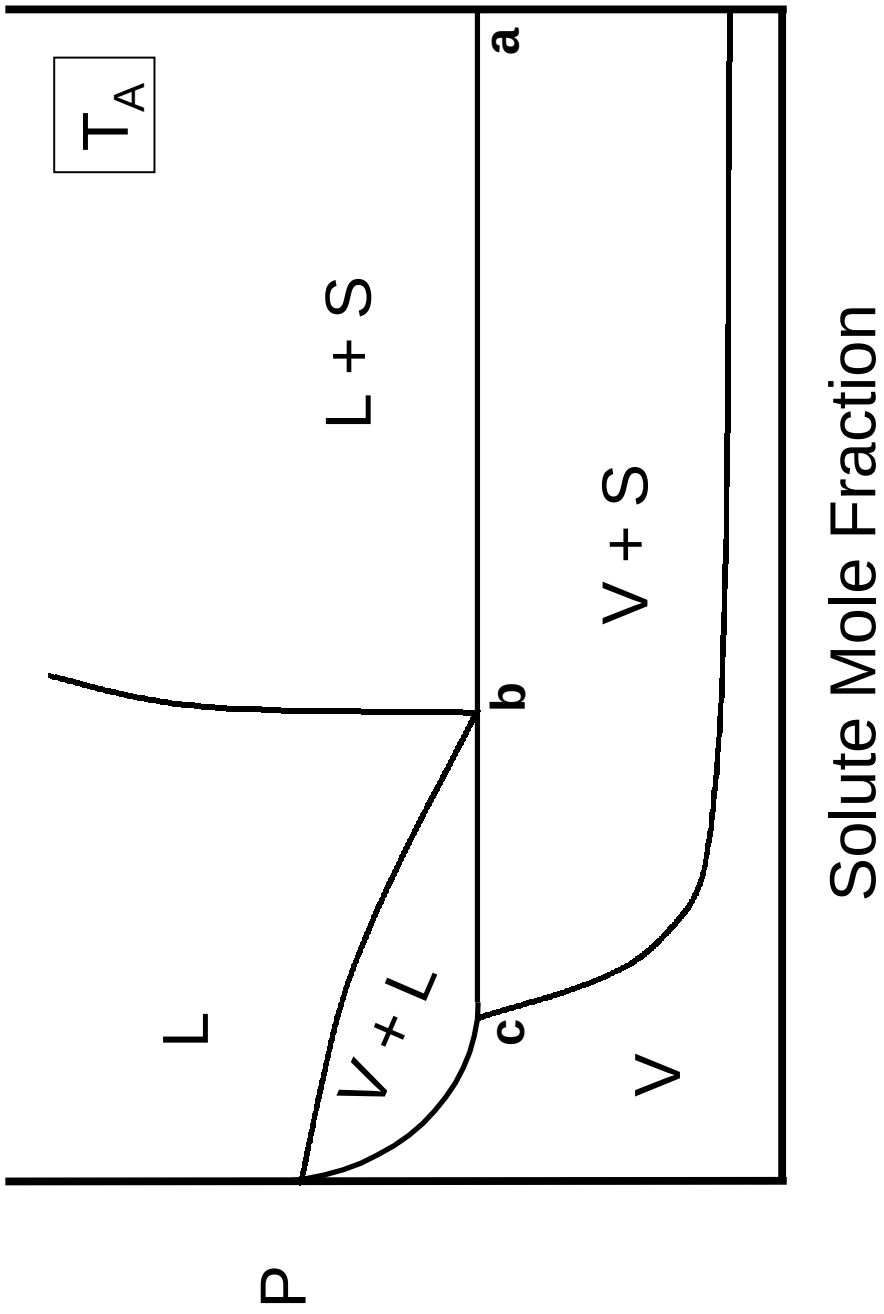

Figure 2: Pressure-composition diagram at temperature T_{A} in Figure 1. See text for discussion.

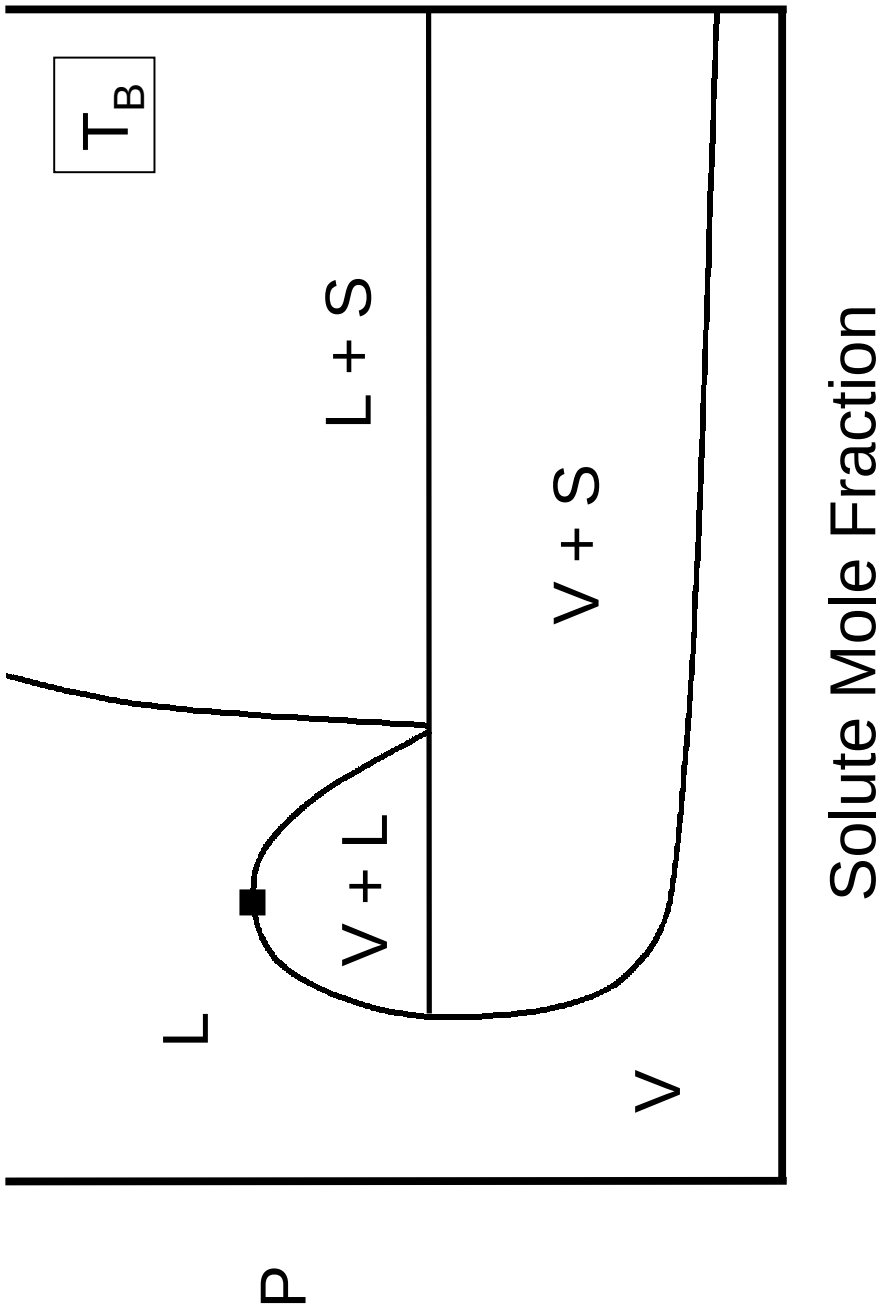

Figure 3: Pressure-composition diagram at temperature T_{B} in Figure 1. See text for discussion.

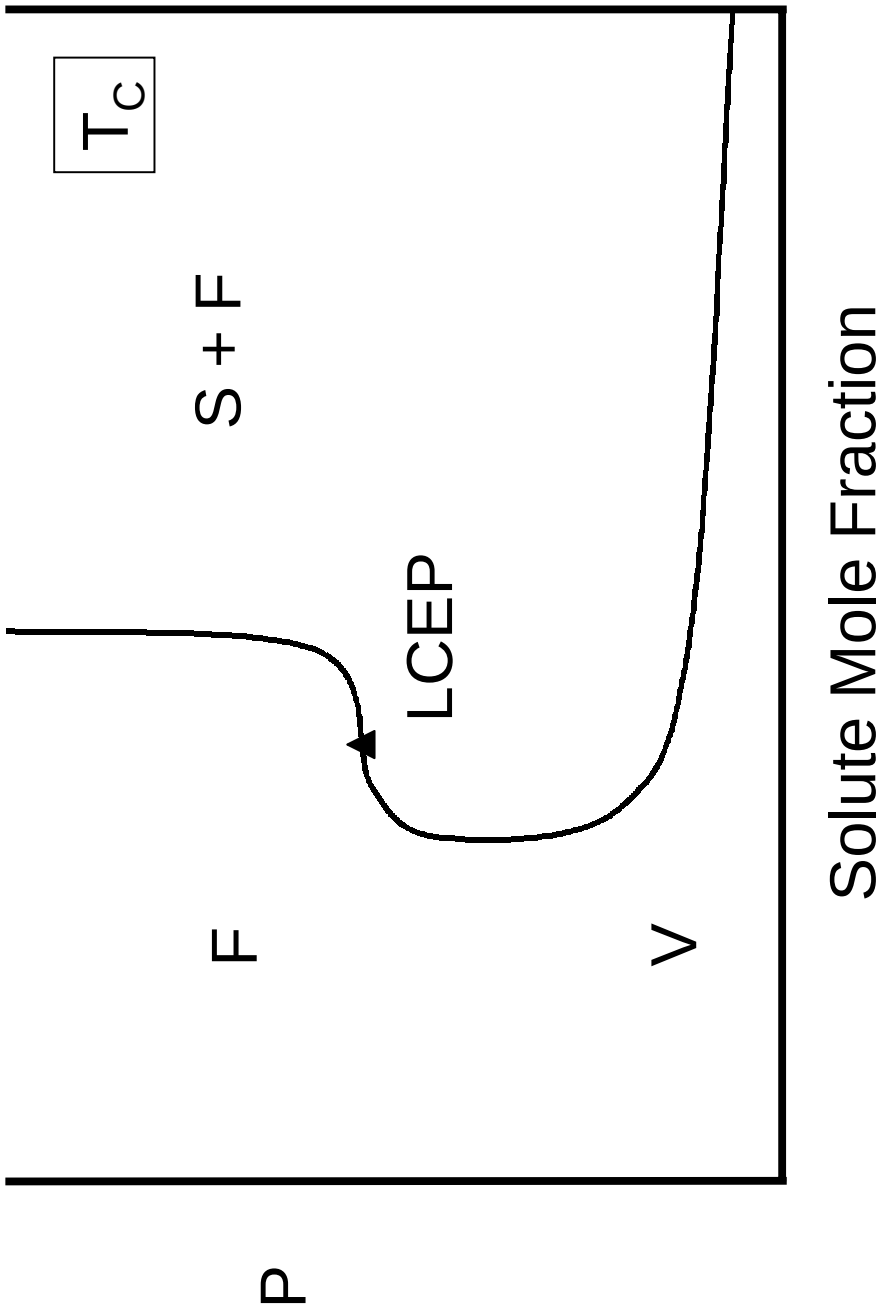

Figure 4: Pressure-composition diagram at temperature T_{C} in Figure 1. See text for discussion.

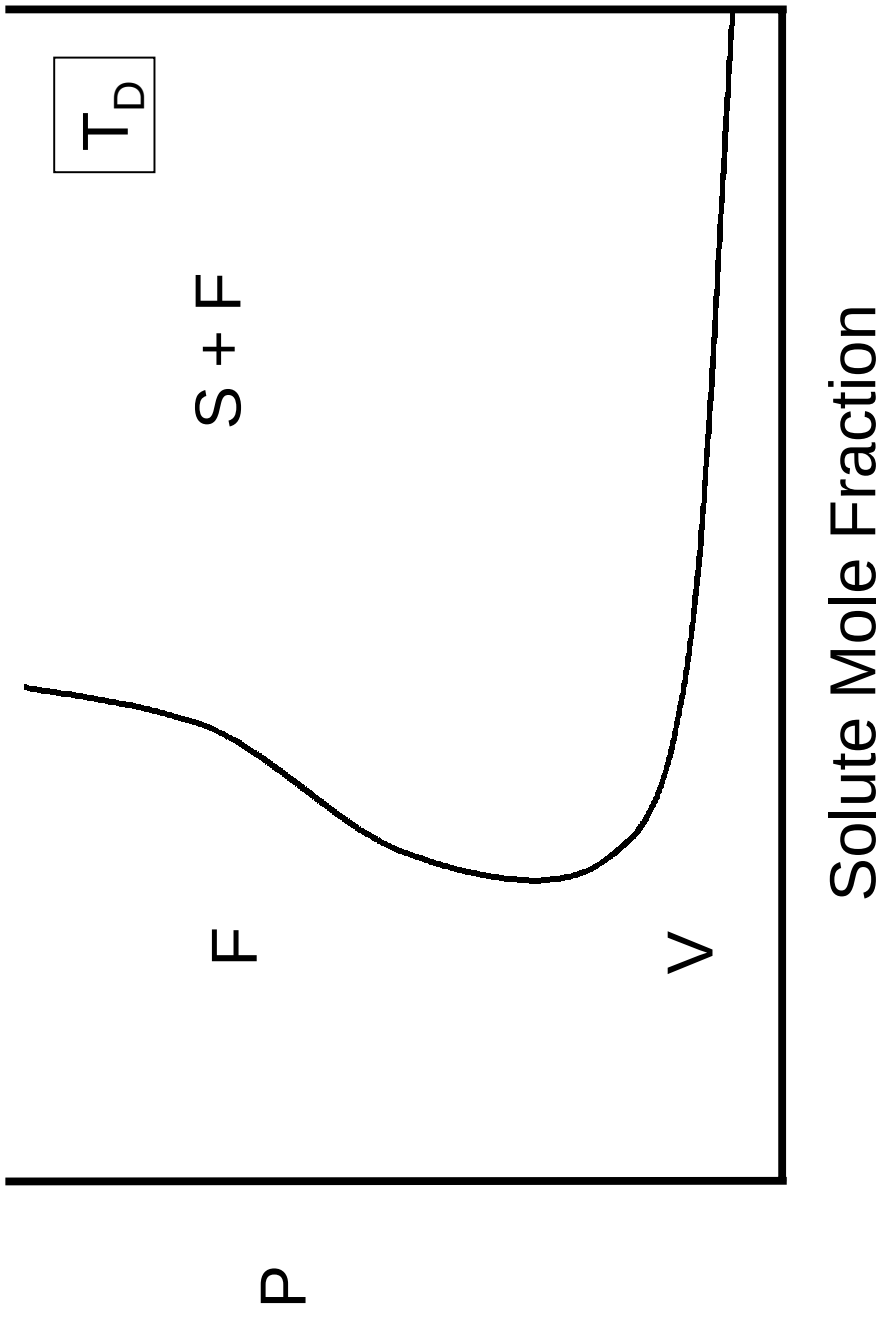

Figure 5: Pressure-composition diagram at temperature T_{D} in Figure 1. See text for discussion.

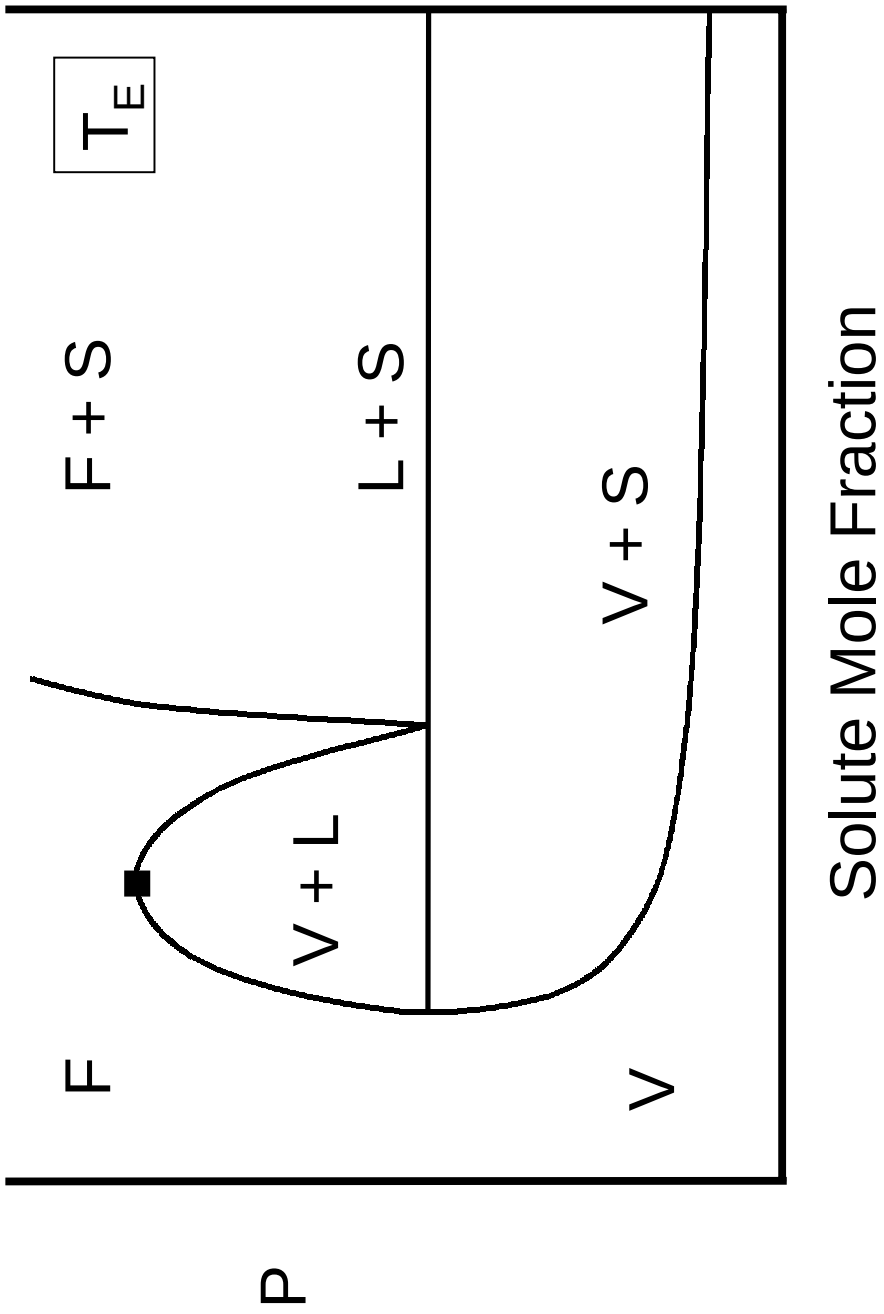

Figure 6: Pressure-composition diagram at temperature T_{E} in Figure 1. See text for discussion.

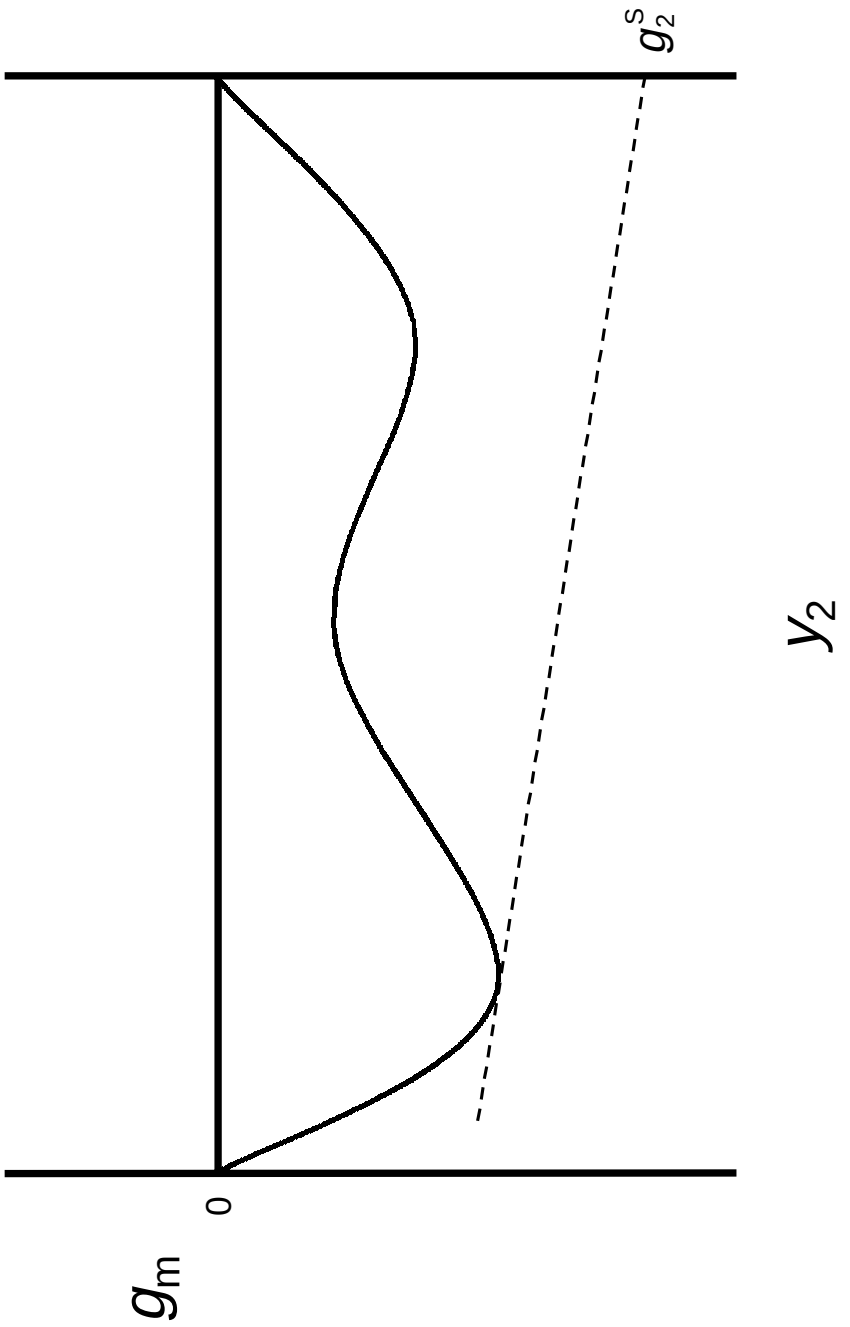

Figure 7: Hypothetical plot of Gibbs energy of mixing g_{m} vs. solubility y_2, showing a situation in which there is only one root to the equifugacity condition. g_2^{S} indicates the Gibbs energy of pure solid solute relative to pure fluid solute at the system temperature and pressure.

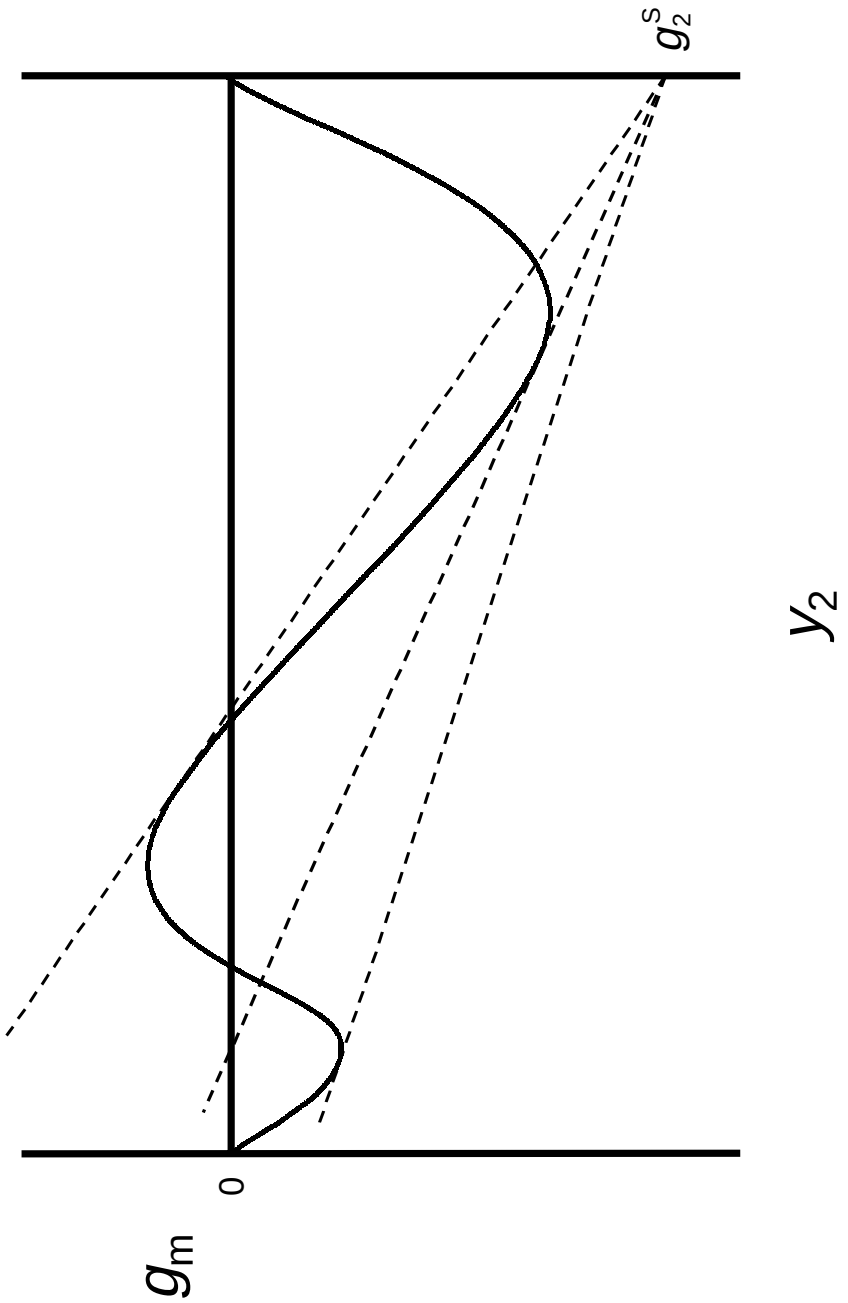

Figure 8: Hypothetical plot of Gibbs energy of mixing g_{m} vs. solubility y_2, showing a situation in which there are three roots to the equifugacity condition. Only the lowest solubility root represents a stable phase. g_2^{S} indicates the Gibbs energy of pure solid solute relative to pure fluid solute at the system temperature and pressure.

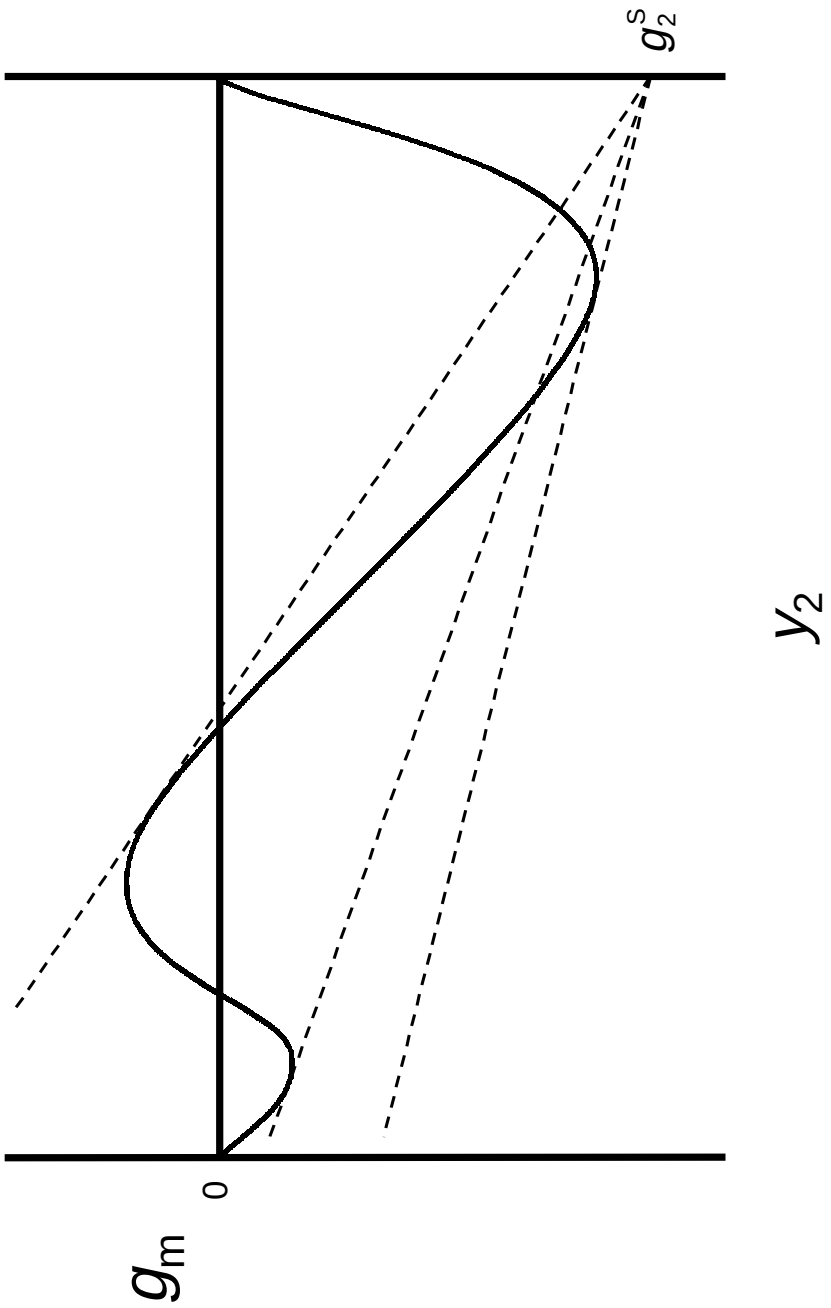

Figure 9: Hypothetical plot of Gibbs energy of mixing g_{m} vs. solubility y_2, showing a situation in which there are three roots to the equifugacity condition. Only the highest solubility root represents a stable phase. g_2^{S} indicates the Gibbs energy of pure solid solute relative to pure fluid solute at the system temperature and pressure.

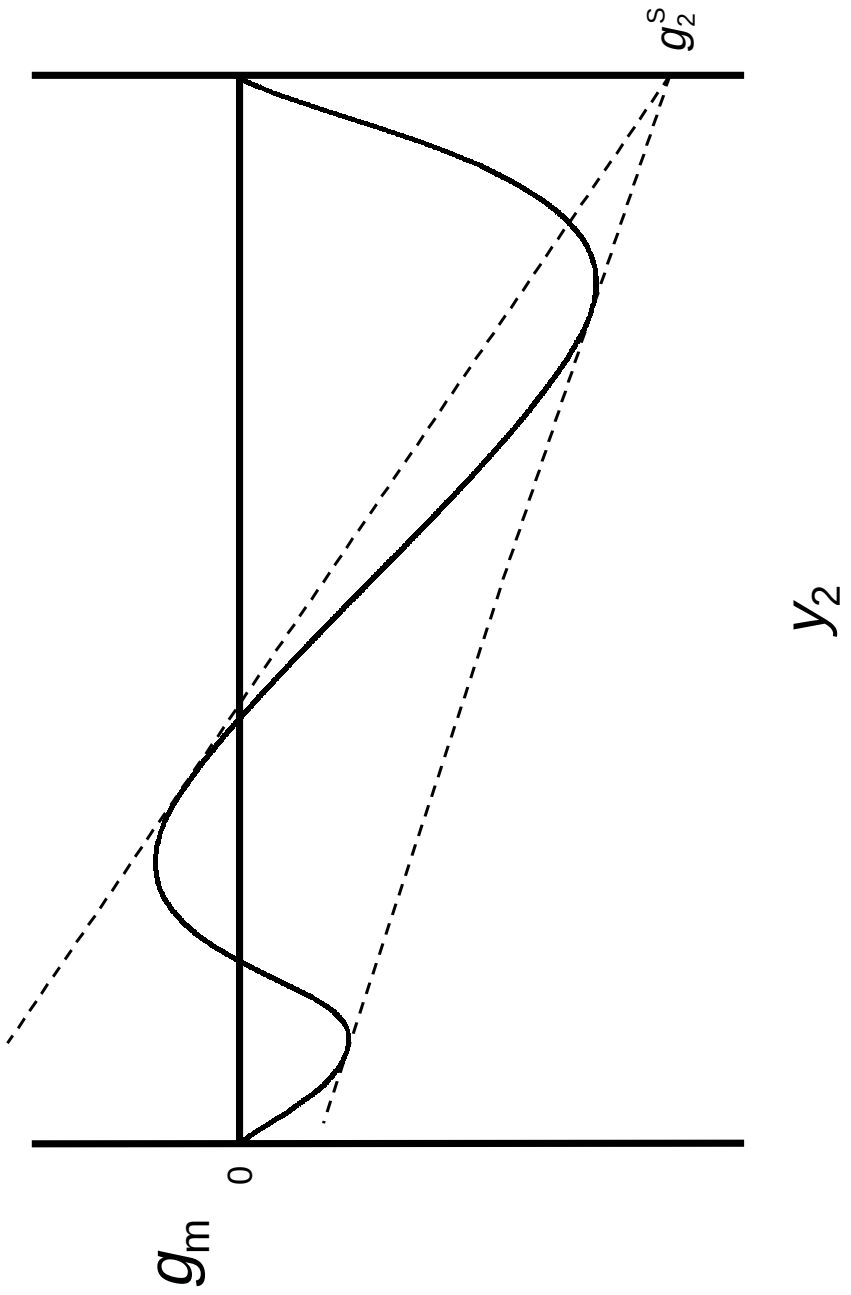

Figure 10: Hypothetical plot of Gibbs energy of mixing g_{m} vs. solubility y_2, showing a situation in which there are three roots to the equifugacity condition. Here both the lowest and highest solubility roots represents stable phases, indicating solid-liquid-vapor equilibrium. g_2^{S} indicates the Gibbs energy of pure solid solute relative to pure fluid solute at the system temperature and pressure.

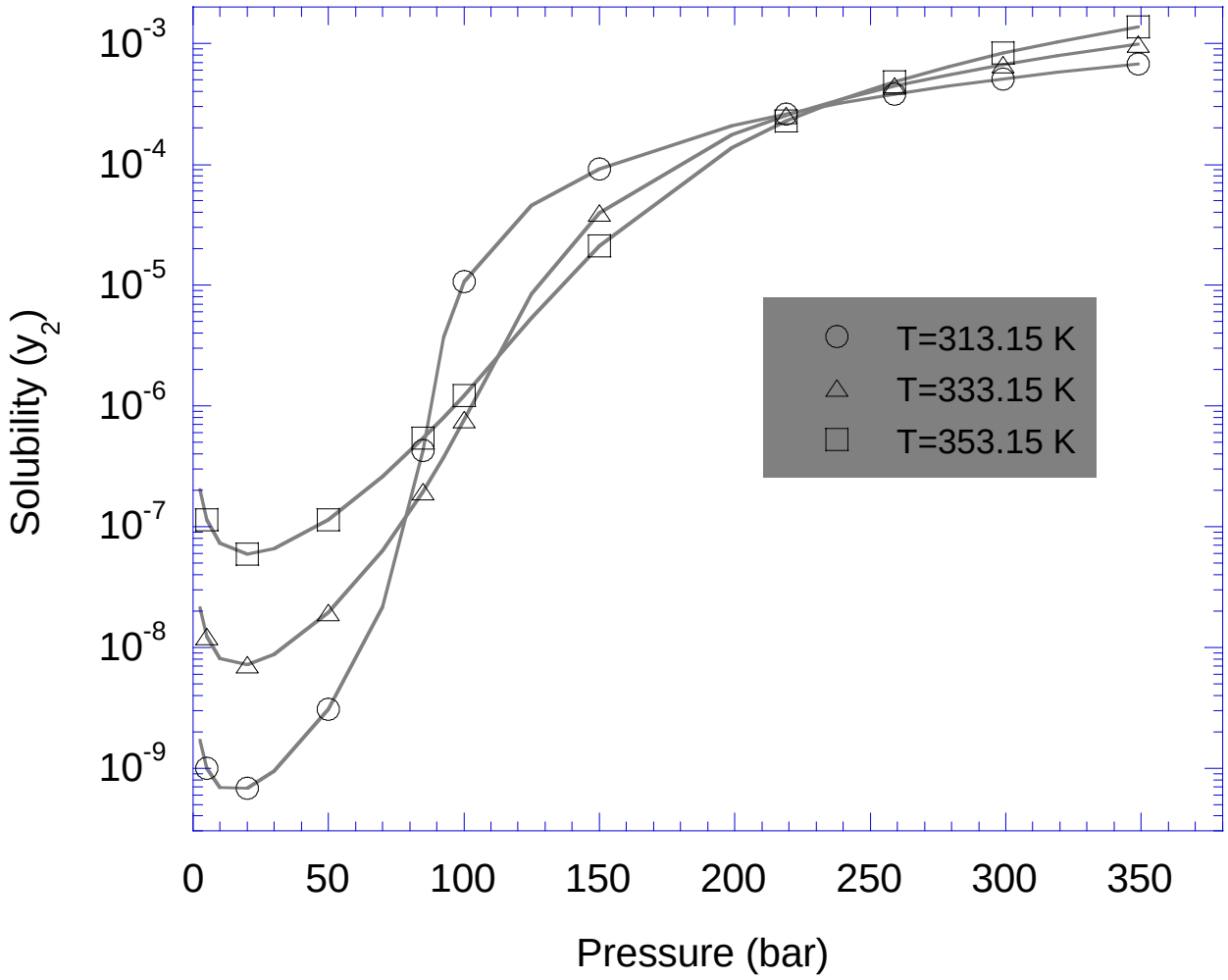

Figure 11: Computed equifugacity roots for Example 1, showing the solubility of caffeine in CO_2. There is only one equifugacity root at each temperature and pressure considered, and that root corresponds to stable solid-fluid equilibrium.

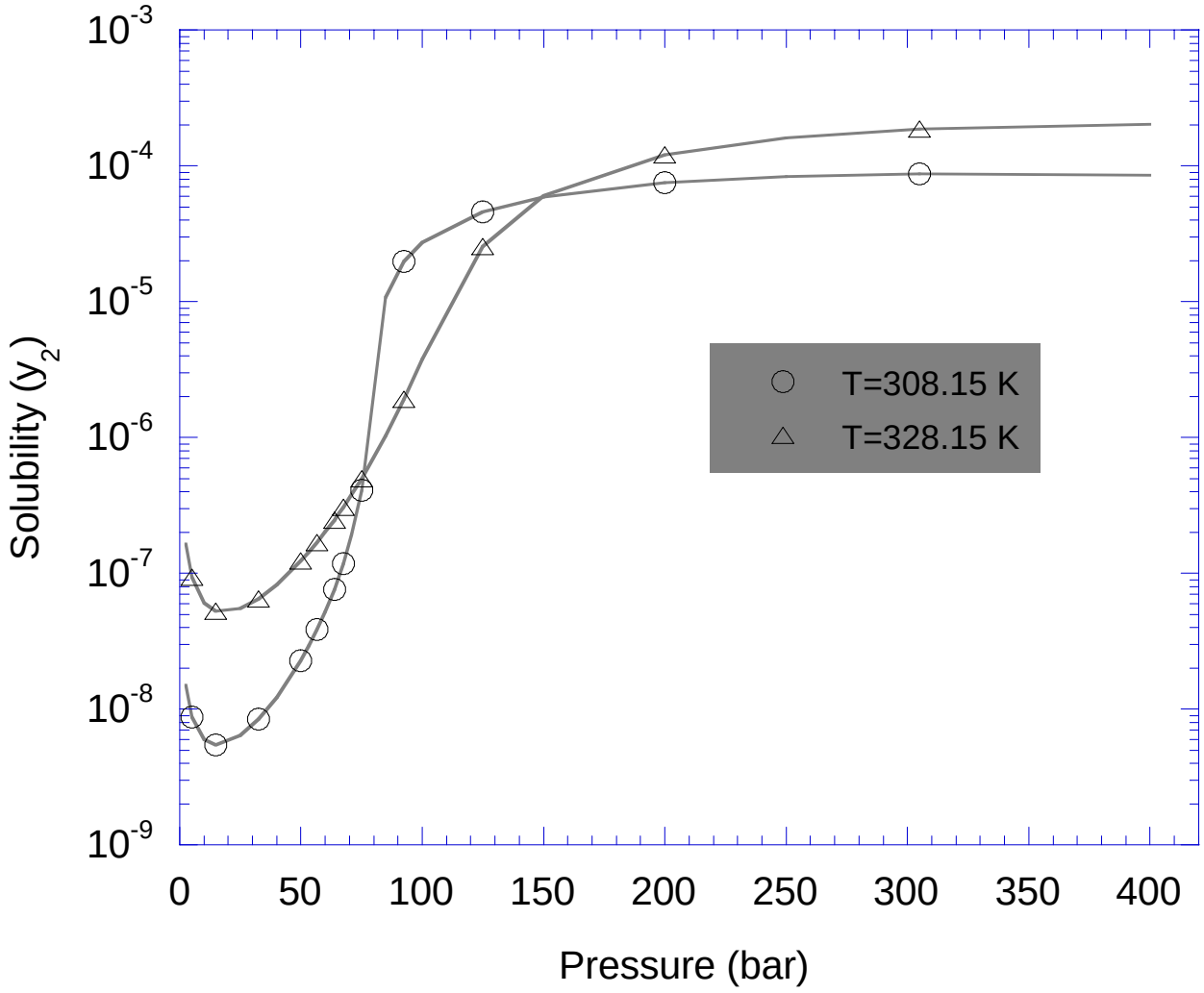

Figure 12: Computed equifugacity roots for Example 2, showing the solubility of anthracene in CO_2. There is only one equifugacity root at each temperature and pressure considered, and that root corresponds to stable solid-fluid equilibrium.

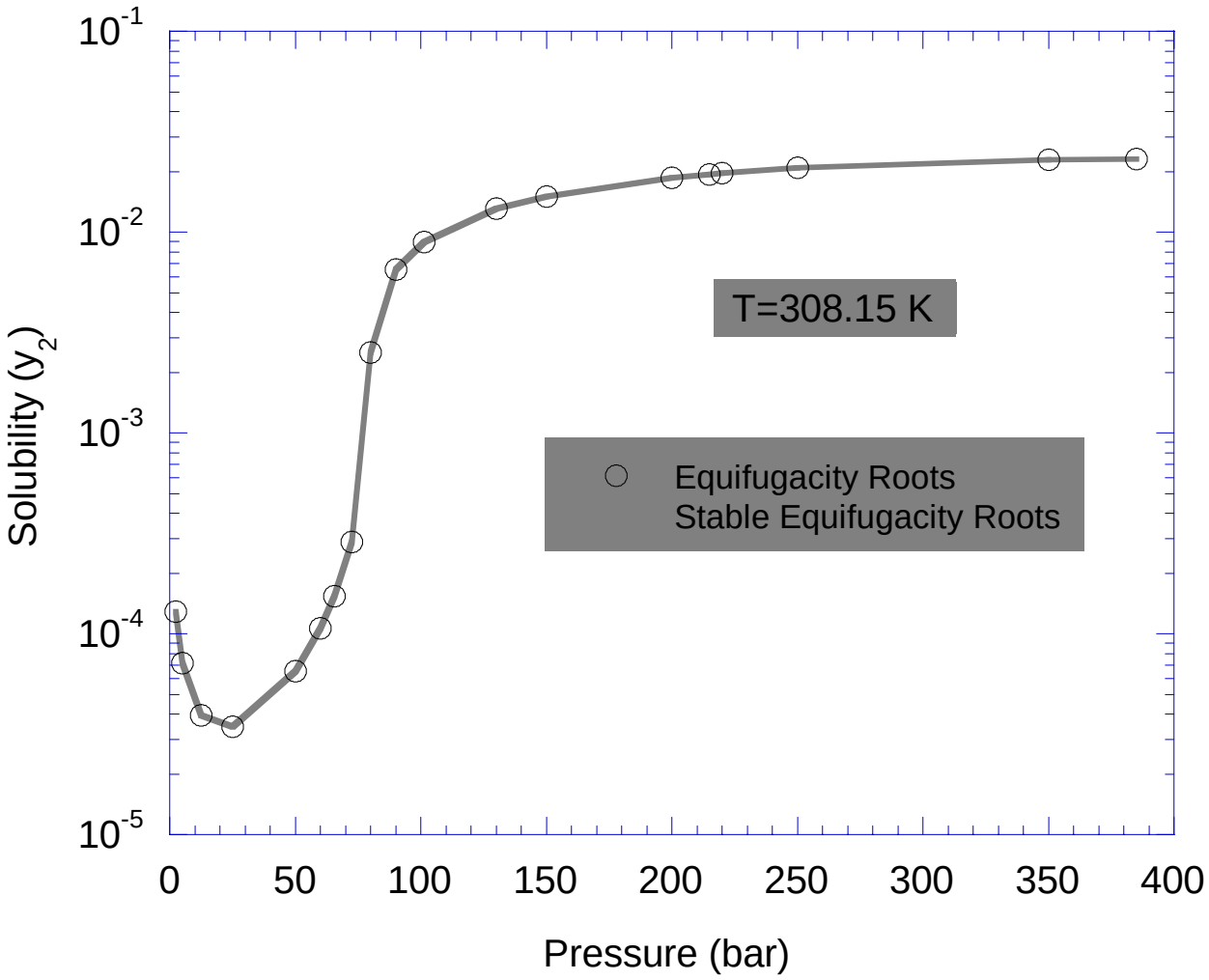

Figure 13: Computed equifugacity roots for Example 3, showing the solubility of naphthalene in CO_2 at 308.15 K. At this temperature, there is only one equifugacity root at each pressure considered, and that root corresponds to stable solid-fluid equilibrium.

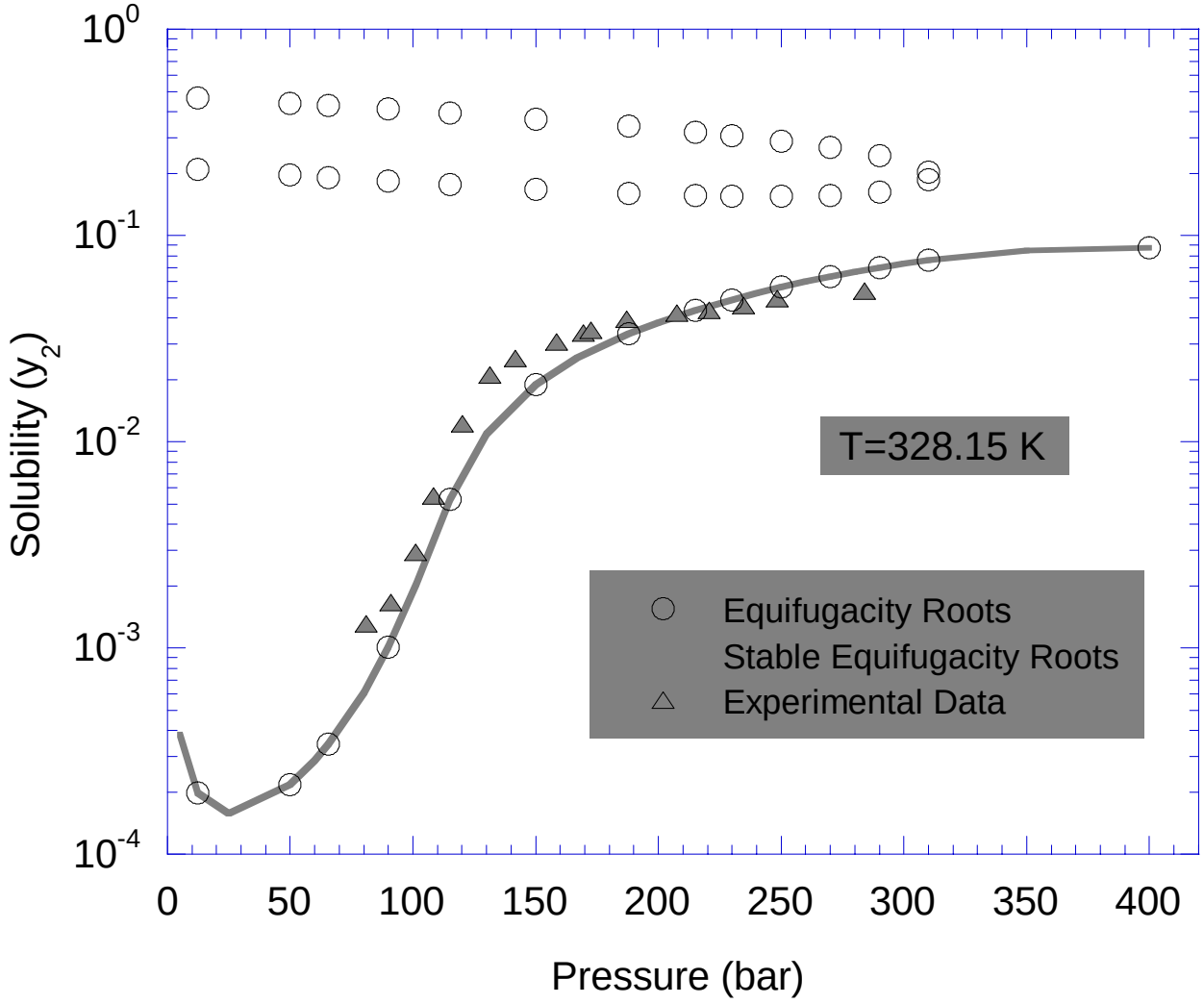

Figure 14: Computed equifugacity roots for Example 3, showing the solubility of naphthalene in CO_2 at 328.15 K. At this temperature, there are multiple equifugacity roots for pressures below about 310 bar. The lowest solubility root always corresponds to stable solid-fluid equilibrium. Experimental data is from McHugh and Paulaitis.[20]

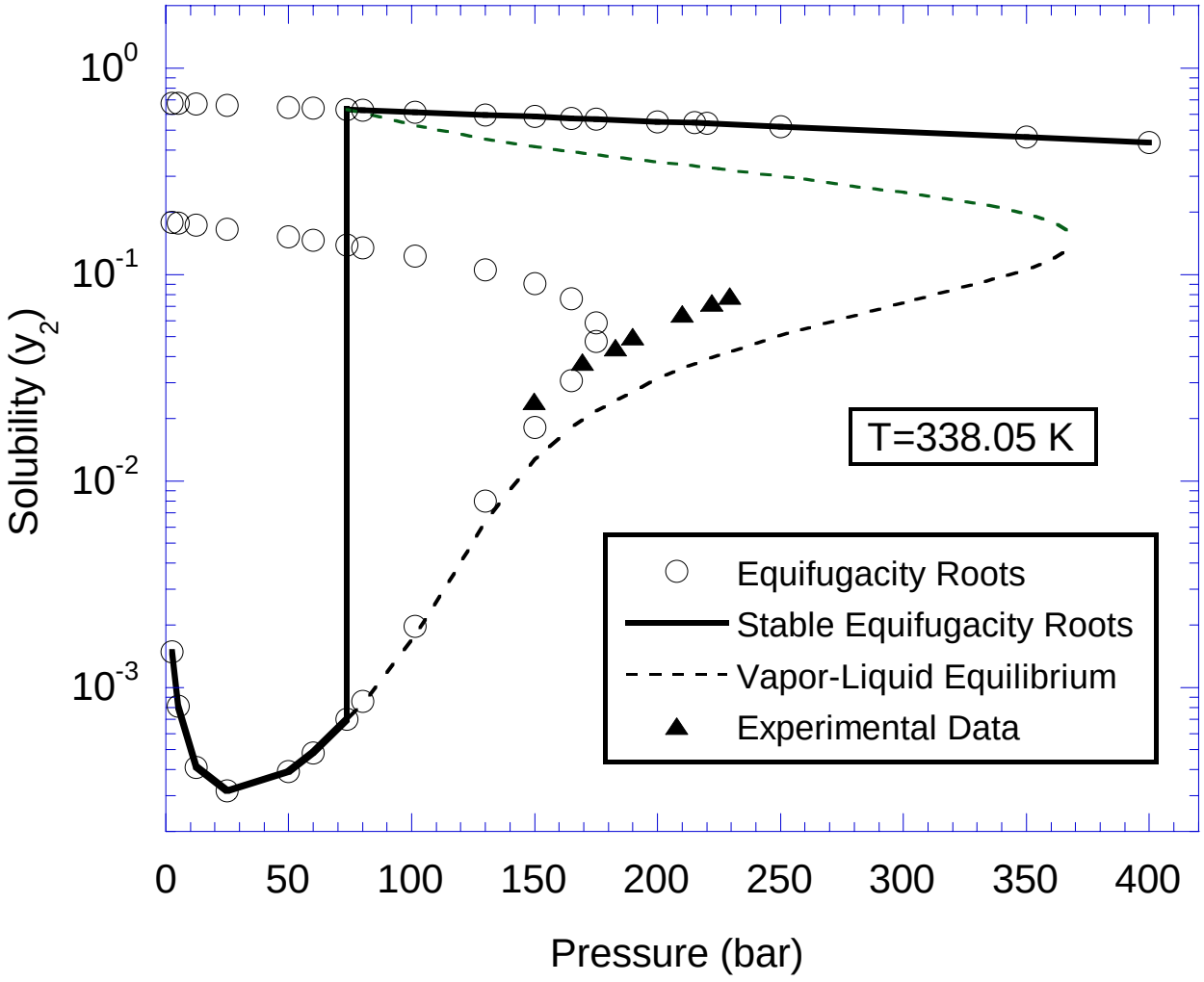

Figure 15: Computed equifugacity roots for Example 3, showing the solubility of naphthalene in CO_2 at 338.05 K. At this temperature, there are multiple equifugacity roots for pressures below about 170 bar. At low pressure the lowest solubility root corresponds to stable solid-fluid equilibrium, but at higher pressure it is the highest solubility root that is stable. A three-phase line (SLV) occurs at about 73.60 bar. The experimental data of McHugh and Paulaitis[20] was originally reported as solid-fluid, but clearly is not. See text for further discussion.

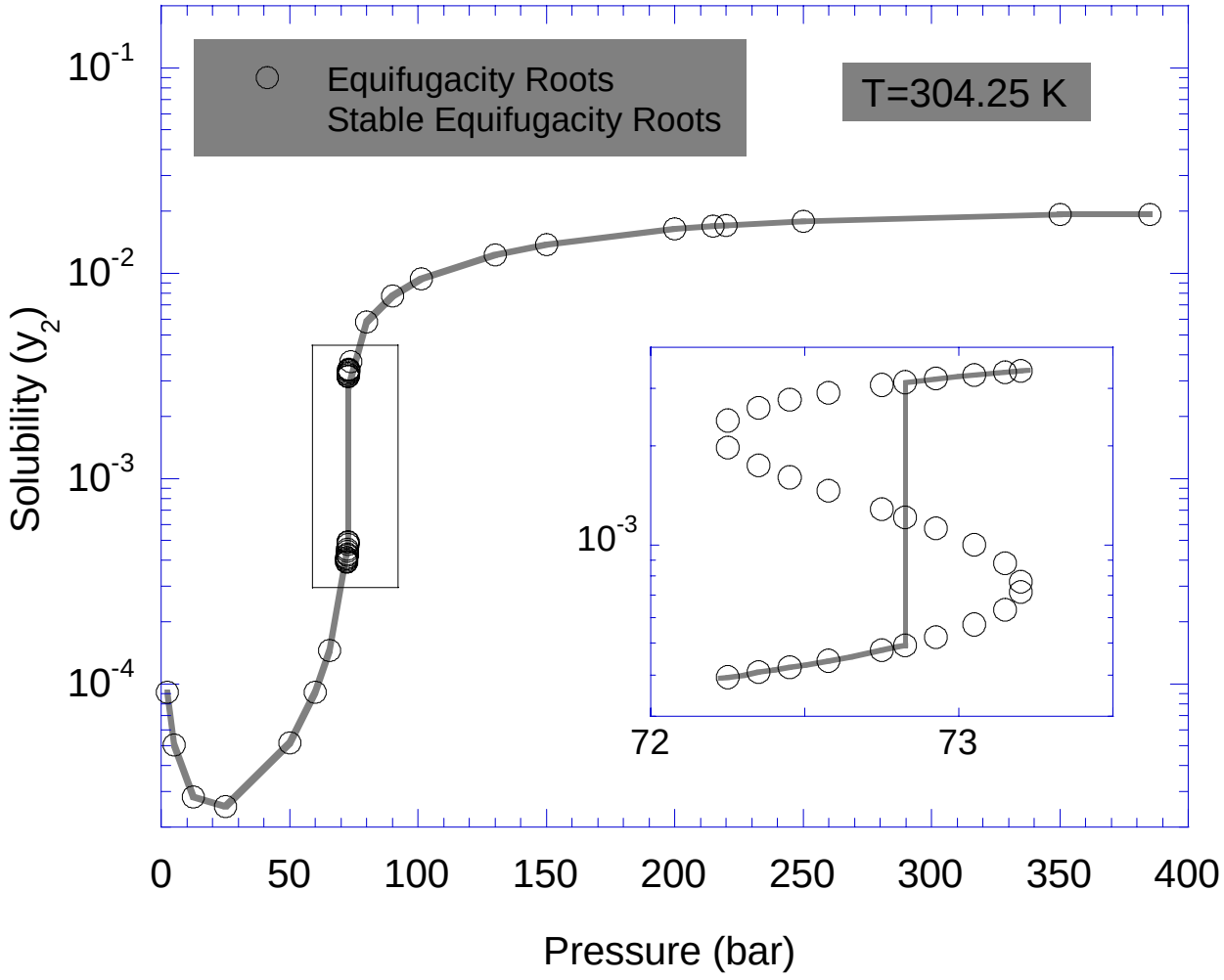

Figure 16: Computed equifugacity roots for Example 3, showing the solubility of naphthalene in CO_2 at 304.25 K. The portion of the curve enclosed in the box is enlarged in the inset to its right. At this temperature, there are multiple equifugacity roots for a small range of pressures between about 72.2 and 73.2 bar, with a three-phase line (SLV) at about 72.825 bar.

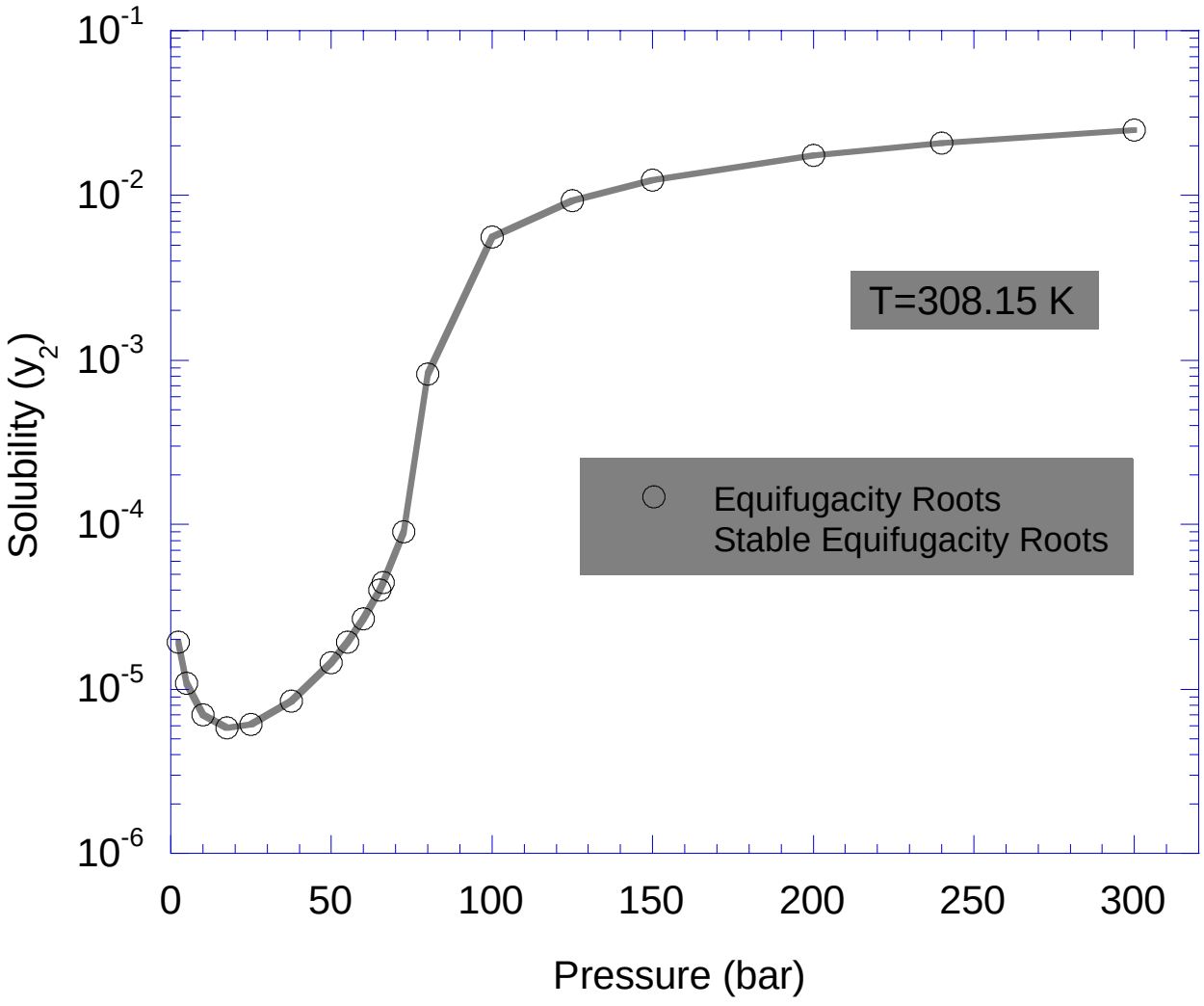

Figure 17: Computed equifugacity roots for Example 4, showing the solubility of biphenyl in CO_2 at 308.15 K. At this temperature, there is only one equifugacity root at each pressure considered, and that root corresponds to stable solid-fluid equilibrium.

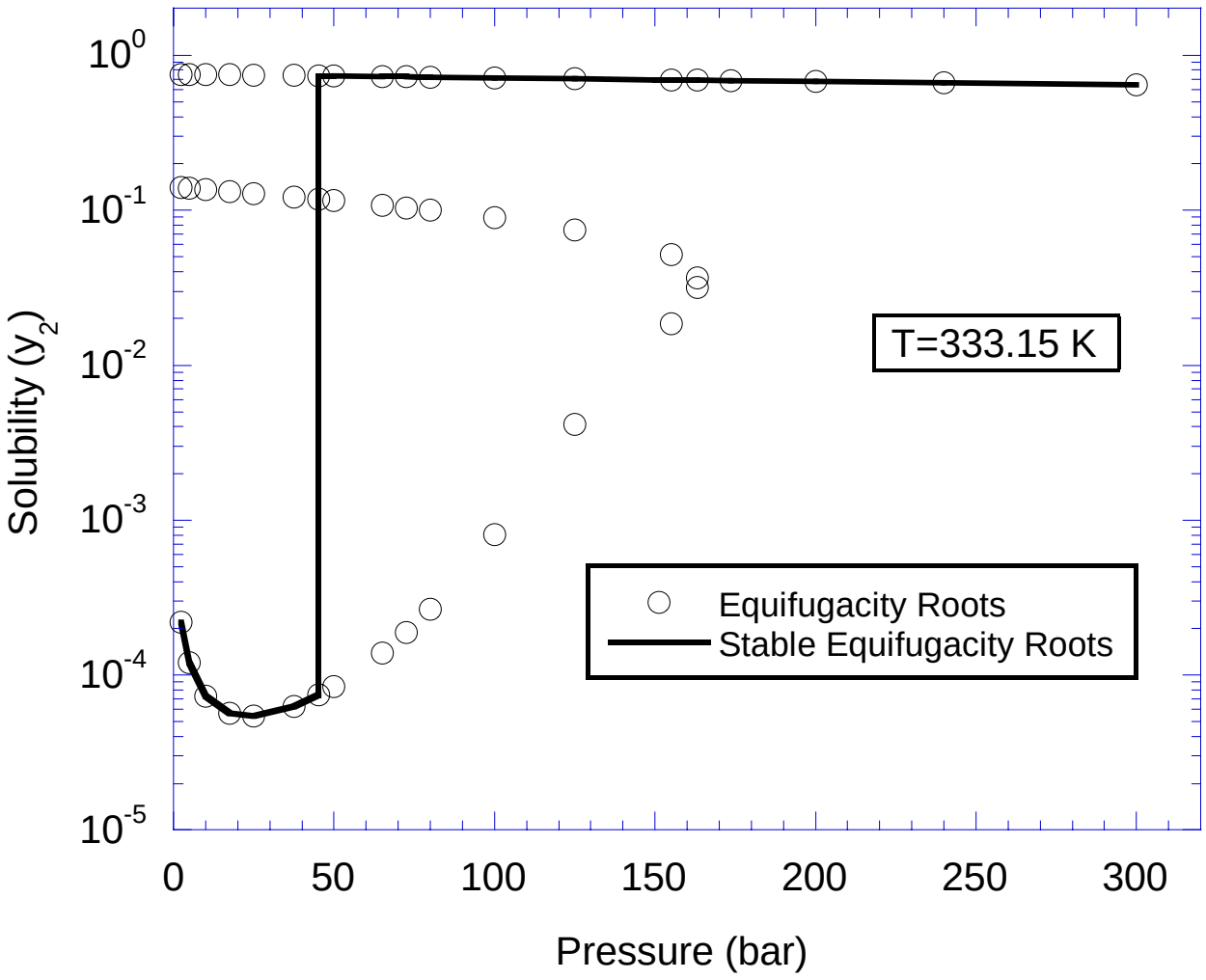

Figure 18: Computed equifugacity roots for Example 4, showing the solubility of biphenyl in CO_2 at 333.15 K. At this temperature, there are multiple equifugacity roots for pressures below about 160 bar. At low pressure the lowest solubility root corresponds to stable solid-fluid equilibrium, but at higher pressure it is the highest solubility root that is stable. A three-phase line (SLV) occurs at about 45.19 bar.

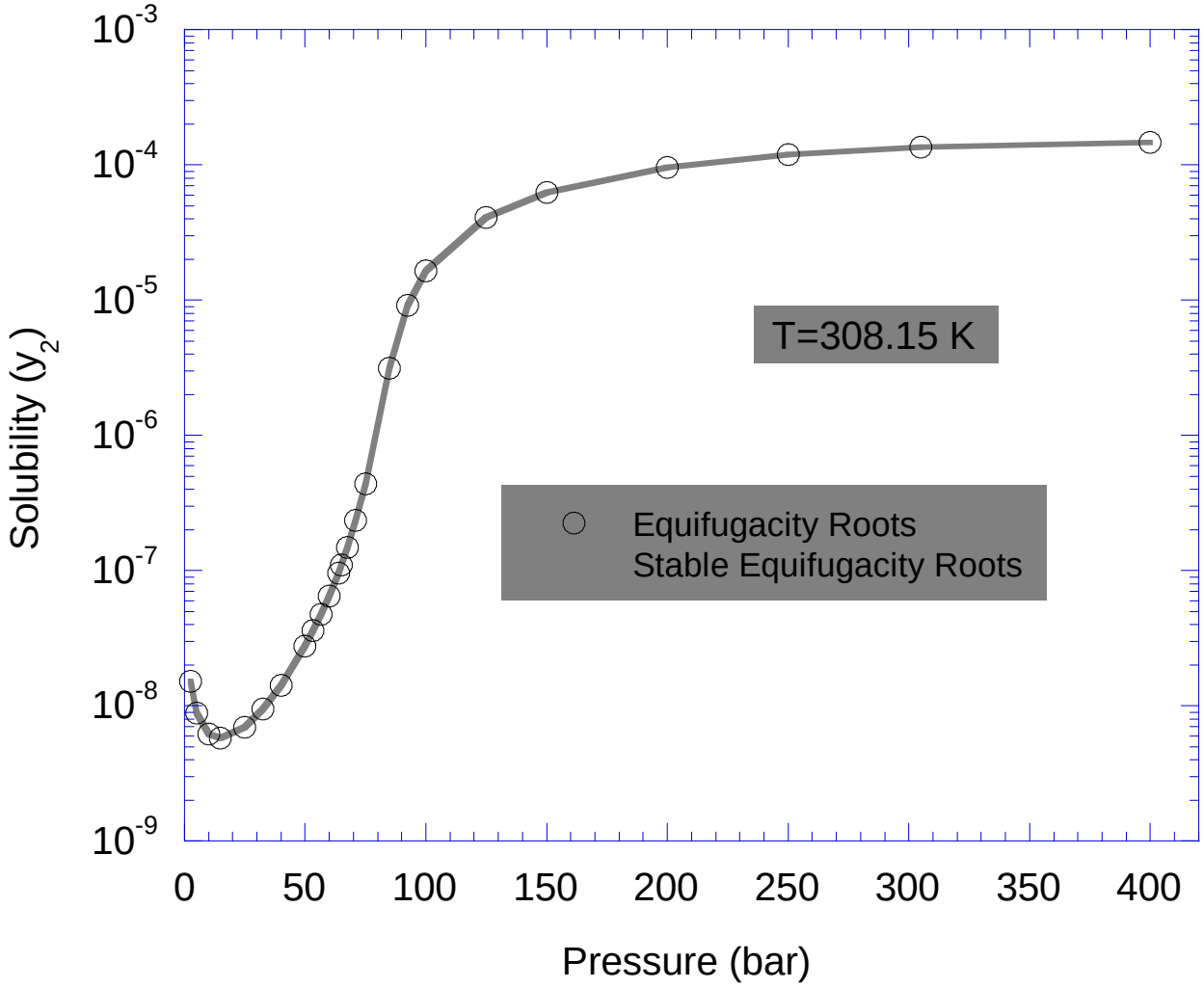

Figure 19: Computed equifugacity roots for Example 5, showing the solubility of anthracene in a mixed solvent of 5:1 (molar) CO_2 and ethane at 308.15 K. At this temperature, there is only one equifugacity root at each pressure considered, and that root corresponds to stable solid-fluid equilibrium.